IEEE Access
Multidisciplinary ⋮ Rapid Review ⋮ Open Access Journal

Received December 2, 2019, accepted December 28, 2019, date of publication January 3, 2020, date of current version January 14, 2020.

Digital Object Identifier 10.1109/ACCESS.2020.2963843

Active Control for Wall Drag Reduction: Methods, Mechanisms and Performance

LU ZHANG, XIAOBIAO SHAN, AND TAO XIE
State Key Laboratory of Robotics and System, Harbin Institute of Technology, Harbin 150001, China
Corresponding authors: Xiaobiao Shan (shanxiaobiao@hit.edu.cn) and Tao Xie (xietao@hit.edu.cn)

This work was supported in part by the National Natural Science Foundation of China under Grant 51677043.

ABSTRACT Active reducing the skin friction drag of vehicles (such as missiles, rockets, aircraft, high-speed train, submarines, etc.) during the navigation process can improve the respond speed effectively, save the energy consumption and increase the endurance time. As lots of active drag reduction methods were proposed for different applications, a review article is urgently needed to guide researchers to choose suitable methods for their pre-research. In this review, the generation mechanisms of skin friction drag under the action of disturbing the turbulent boundary layer are discussed, and the main active drag reduction methods are summarized. According to the actuation modes, we divided the active drag reduction methods into: drag reduction based on wall motion; drag reduction based on volume force control; drag reduction based on wall deformation and drag reduction based on micro vibration generated by piezoelectric actuator. The development status, drag reduction mechanisms, typical structures and drag reduction performance of each active drag reduction method are discussed and summarized in this work, which can provide preliminary research references for those who are engaged in the research of active wall drag reduction.

INDEX TERMS Drag reduction, active control methods, piezoelectric actuator, skin friction drag, turbulent boundary layer.

I. INTRODUCTION

Due to the impact of the oil crisis in the early 1970s, the drag reduction technology has developed gradually in recent decades. Especially in the field of military and transport, achieving drag reduction can not only reduce energy consumption so as to improve the total navigation time, but also increase the sailing speed to meet the strategic requirements of rapid response, as shown in Fig.1. Researches shown that, for vehicles driving in air or sea, much energy could be saved when little skin friction drag was reduced [1], [2]. Thus, effective drag reduction technology is of great significance to improve the performance of vehicles and save energy.

For objects moving in fluids (air, water, etc.), skin frictional drag is mainly generated in the region where turbulence occurs, and can be adjusted by controlling the characteristics of the near wall turbulent boundary layer. Therefore, the effective turbulence control methods have attracted extensive attention of researchers in the past decades [3], [4]. By controlling the turbulent boundary layer, we can achieve: (a) drag reduction [5], (b) flow pressure fluctuation controlling [6], [7], (c) flow separation controlling [8]–[11], (d) transition controlling [12]–[14], (e) lift adjusting [15], [16], (f) noise suppression [17]–[19], and so on. Here, we mainly discuss the effective methods of controlling the coherent structure of the near wall turbulent boundary layer for reducing the skin frictional drag.

Varies of passive and active control methods for drag reduction has been proposed after that the riblet drag reduction method was proved to be effective in reducing the skin friction drag [20], [21]. Passive control methods are mainly used in some specific conditions, and the controlling parameters generally remain unchanged. Active control methods can be applied in common conditions where the characteristics of the turbulent boundary layer are variable, and have developed rapidly in recent years. Deng et al. [22] achieved skin friction drag reduction by using the opposition active control method (wall blowing and suction), and studied the drag reduction characteristics when the method was applied in fluid with different Reynolds numbers. Xiang *et al.* [23] proposed the method of achieving drag reduction by using cavitation hydrofoil, and the Bubble-Droplet cavitation model

The associate editor coordinating the review of this manuscript and approving it for publication was Gursel Alici.

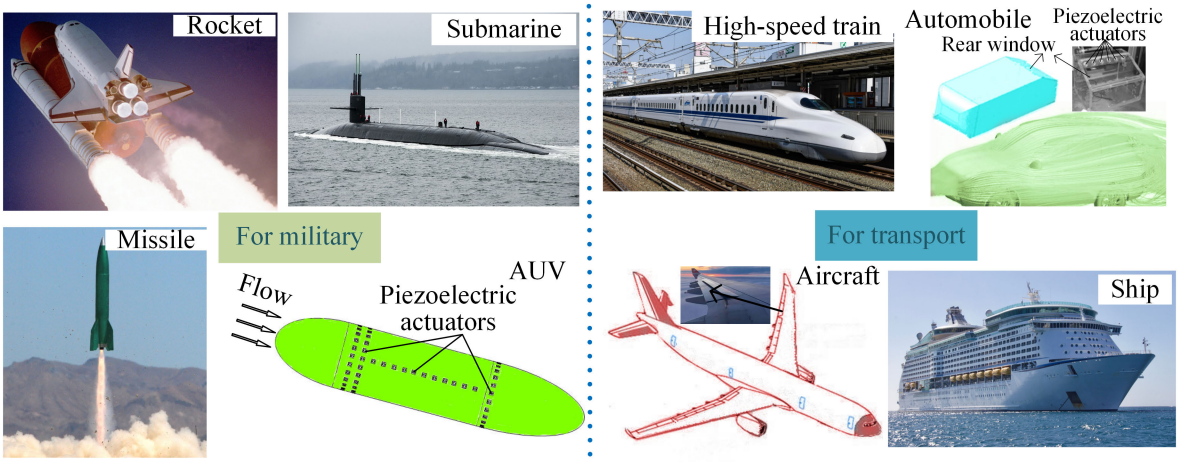

FIGURE 1. Application fields of drag reduction.

was established to study the unsteady dynamics of Clark-y cavitating hydrofoil.

In this work, the mechanisms, characteristics, research status and application fields of active drag reduction technologies with different actuation modes are mainly discussed. Firstly, in section 2, the generation process of coherent structure in near wall turbulent boundary layer and how the skin friction drag is influenced by the turbulent coherent structure are illustrated. Then, in section 3, the effective active control methods and the corresponding working mechanisms for reducing the skin friction drag by modifying coherent structure are introduced. The actuation modes of the control methods mainly include wall motion, volume force control of near wall fluid, wall deformation and micro vibration produced by piezoelectric actuator. The drag reduction methods based on micro vibration have the advantages of simple structure, low power consumption and high drag reduction rate, are emphatically discussed in this section. Finally, in section 4, conclusions are summarized based on the discussion results and some feasible proposes are given for the future follow up studies of corresponding drag reduction control methods.

II. TURBULENT COHERENT STRUCTURE AND FRICTION DRAG REDUCTION

According to the Prandtl boundary layer equations, when fluid flows on the surface of an object, the friction force mainly created in the thin layer of fluid adjacent to the wall. This thin layer of fluid is termed as the turbulent boundary layer and it exists in most actual flow fields. With the development of detection technology and statistical analysis technology of fluid characteristics, the structure of boundary layer is gradually revealed. As shown in Fig.2, the turbulent boundary layer consists of inner layer and outer layer, inner layer is mainly composed of the sublayer, the buffer layer, and the logarithmic layer.

Although the turbulent interactions exist between the inner layer and outer layer, drag reduction can be achieved by mainly controlling the inner layer [24]–[26].

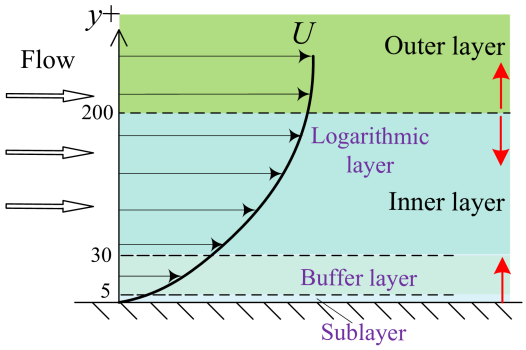

FIGURE 2. The structure of turbulent boundary layer.

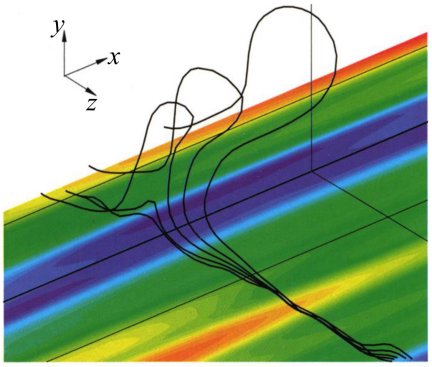

FIGURE 3. Vortex structures and instantaneous streamwise velocity contours ($Re = 150$) [36]. Blue and red indicate low-speed streaks and high-speed streaks respectively; the black lines denote vortex lines.

There are various kinds of vortices existing in the near wall fluid, among which horseshoe and hairpin vortices are the key factors to generate turbulence [27]–[29]. The generation of turbulent motion depends mainly on the characteristics of sublayer ($0 < y^+ < 5$) and the buffer layer ($5 < y^+ < 30$), where y^+ is the dimensionless normal distance from the wall. The velocity of fluid in viscous sublayer and buffer layer presents streak structure (high-speed region and low-speed region appear alternatively), as shown in Fig.3.

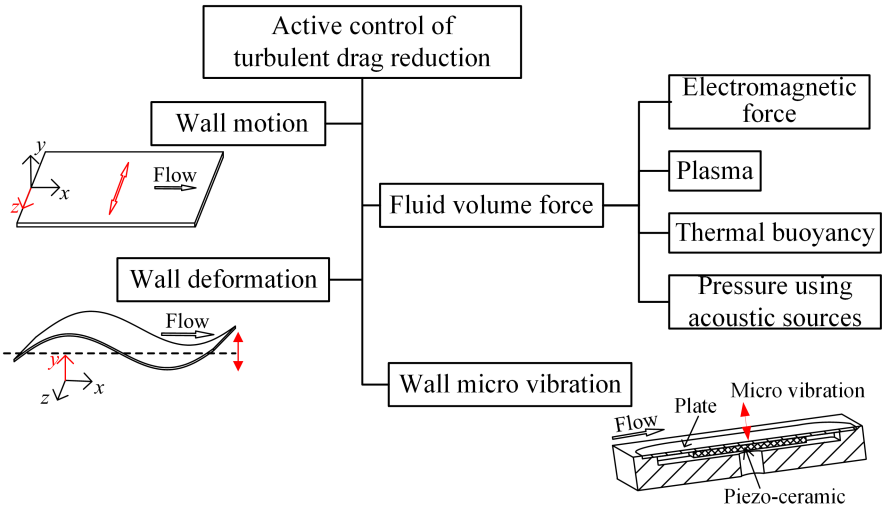

FIGURE 4. Classification of active control for turbulent drag reduction.

Low-speed fluids eject from the wall to the outside, while high-speed fluids sweep from the outside to the wall [30], [31]. The ejection and sweep processes are mainly induced by inclined quasi-streamwise vortices which are the main cause of Reynolds stress [32]. As this processes mainly occur in the near wall region ($y^+ < 15$), which means that the near wall control methods are easy to achieve drag reduction [33]–[35].

The interaction between various kinds of vortices and high/low speed streaks constitutes turbulent coherent structure in the near wall region. The periodicity of coherent structure plays an important role in the self-sustainment of turbulent boundary layer [37]–[40]. The ejection and sweep processes in the near wall fluid redistribute the velocity gradient and change the Reynolds shear stress, thus forming new alternating high and low speed streaks. The generation mechanism of streamwise vortices can generally be described as that the parent vortices produce the offspring vortices in the near wall field [41], [42], or the high/low speed streaks produce streamwise vortices due to the instability of shear layer [43]–[45]. Bernard *et al.* [42] studied the dynamic evolution of near-wall quasi-streamwise vortices, and found that the generated Reynolds shear stress is beneficial to the formation of new vortices in turbulent boundary layer. It can be seen that the self-sustainment of the turbulent boundary layer is the main factor causing the skin friction force near the wall.

Controlling the turbulent coherent structure artificially and disturbing the self-sustainment of turbulent boundary layer can restrain the turbulent bursting and reduce the wall resistance. Deng and Xu [46] reduced skin friction force by controlling the generation of quasi-streamwise vortices near the wall. Endo *et al.* [47] achieved a drag reduction rate of 12% by weakening the streamwise vortices near the wall. Kravchenko *et al.* [48] obtained the relationship between the wall shear rate and the streamwise vortices near the wall, and found that the measuring position had a great influence on the wall friction resistance. Kim and Lee [49] found that the decrease of skin friction force was accompanied by the decrease of the amount of quasi-streamwise vortices by controlling streamwise stress.

In order to control the turbulent coherent structure effectively to achieve drag reduction, various active control methods are proposed by researchers. According to the action modes for disturbing the turbulent boundary layer, the main active control methods can be divided as: drag reduction based on wall motion, drag reduction based on volume force control, drag reduction based on wall deformation, and drag reduction based on micro vibration, as shown in Fig.4. Drag reduction based on wall motion is achieved by controlling wall motion to interfere with the characteristics of the turbulent boundary layer. Drag reduction based on force control is achieved by directly disturbing the near wall turbulent boundary layer by applying volume force (such as electromagnetic force, plasma force, etc.) to the near wall fluid. Drag reduction based on wall deformation is obtained by using external force to drive the wall to deform along the normal direction, thus interacting with the turbulent boundary layer. Drag reduction based on micro vibration is mainly achieved by using mechanical, electromagnetic and piezoelectric actuators to produce micro vibration on the wall to change the characteristics of the turbulent boundary layer. The mechanisms and drag reduction performance of each control methods are discussed in the following text.

III. DRAG REDUCTION BASED ON WALL MOTION

Drag reduction based on wall motion is an effective method for reducing skin friction drag in turbulent flow [50]–[53]. According to the motion form, it can be divided into drag reduction based on spanwise wall oscillation and drag reduction based on oscillation traveling waves, as shown in Fig.5. For drag reduction based on spanwise wall oscillation,

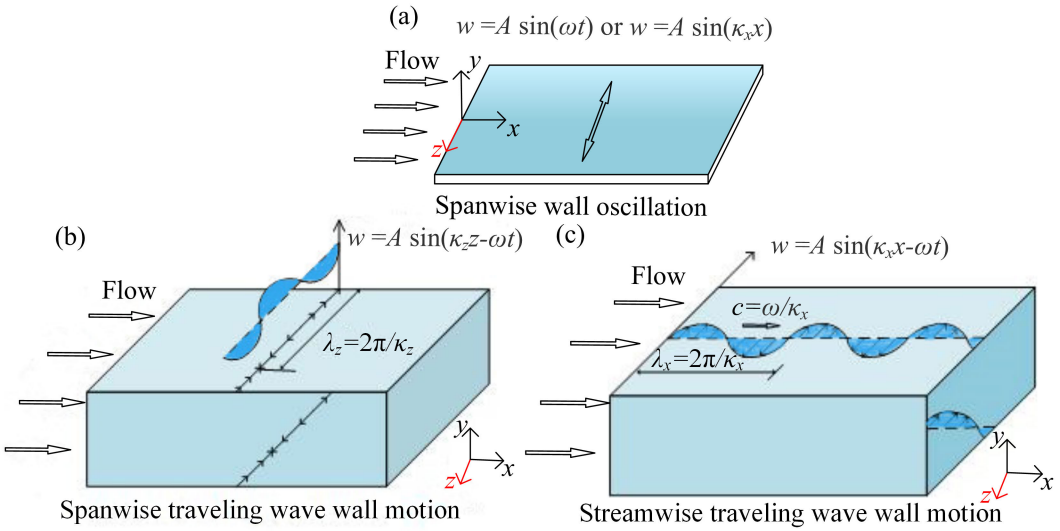

FIGURE 5. The ways of wall motion.

the velocity of wall oscillation is usually a function of time or space (i.e. $w(t) = A\sin(\omega t)$ or $w(x) = A\sin(\kappa_x x)$), as shown in Fig.5(a). For drag reduction based on oscillation traveling waves, the wall oscillation usually propagates in the form of traveling waves along the spanwise direction or along the streamwise direction (i.e. $w(z,t) = A\sin(\kappa_z z - \omega t)$ or $w(x,t) = A\sin(\kappa_x x - \omega t)$), as shown in Fig.5(b) and Fig.5(c). Where A is the amplitude, ω is the angular frequency, κ_x is the streamwise wave number, and κ_z is the spanwise wave number.

A. CREATING SPANWISE WALL OSCILLATION TO ACHIEVE DRAG REDUCTION

Based on the idea that sudden pressure gradient change along the spanwise direction will cause reduction of skin friction drag in turbulent flow [54], Jung *et al.* proposed the method of reducing near-wall drag by high frequency wall oscillation along the spanwise direction. Direct numerical simulation (DNS) results shown that when the dimensionless oscillation period $T^+ = 100$, the turbulence effect in the channel was well suppressed, the Reynolds shear stress and turbulence intensity decreased significantly, and the drag reduction rate was up to 40% [55], [56]. Laadhari *et al.* [57] verified that the mean flow velocity, mean velocity gradient and turbulence intensity of turbulent boundary layer on a flat plate decreased significantly when the spanwise wall oscillation occurred based on experimental results, the experimental setup is shown in Fig.6. Trujillo *et al.* [58] measured the average velocity of the viscous sublayer by means of the hot film technique, obtained a drag reduction rate of 25% and found that wall oscillation could result in the decrease of streamwise velocity fluctuation, normal velocity fluctuation, turbulent shear stress, burst frequency and duration time of turbulence.

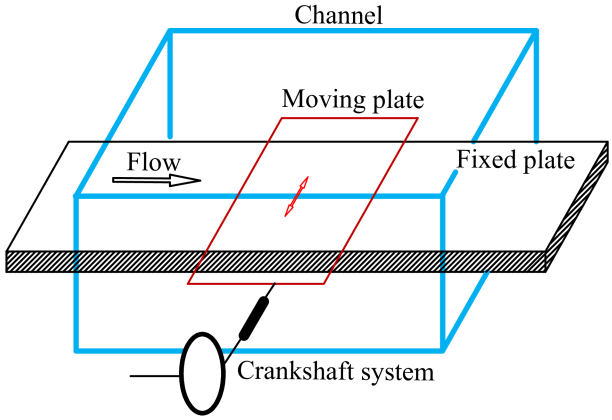

FIGURE 6. Sketch of the experimental setup [57].

The drag reduction effect of wall oscillation is further verified in turbulent pipe flow. Choi and Graham [59] conducted experimental studies on the circular-wall oscillation in a turbulent pipe. The results shown that the friction coefficient can be reduced by 25% by circular-wall oscillation. Quadrio and Sibilla [60] conducted direct numerical simulations of turbulent flow in a pipe, which oscillated along longitudinal axis, and obtained a maximum drag reduction rate of 40%. They thought the main reason was that the oscillation affected the streamwise vortices in the turbulent flow. Duggleby *et al.* [61] carried out relevant researches on wall oscillation of turbulent pipe flow, and the results also demonstrated that wall oscillation of pipe could control the characteristics of near-wall turbulent boundary layer and reduce the skin friction drag.

In addition, Baig et al. studied the drag reduction performance of a cylindrical ring with a super-hydrophobic rotating inner-wall, they found that the Taylor-Couette flows could be formed between the inner and outer walls of the cylindrical ring, and the maximum drag reduction rate could reach up

to 34%. The drag reduction was mainly related to the slip at the wall [62].

In order to obtain higher drag reduction rate, researchers analyzed the influences of related parameters on the drag reduction performance. The key parameters of wall oscillation are oscillation period T, amplitude A, and velocity w. The dimensionless oscillation period can be described as $T^+ = \pi \Delta z^+ / w^+$, where Δz^+ is the dimensionless oscillation amplitude and w^+ is the dimensionless oscillation velocity. Choi *et al.* [63] optimized the oscillation velocity by adjusting the oscillation period and amplitude based on wind tunnel experiments, and a maximum drag reduction rate up to 45% was achieved. They found that the drag reduction rate was proportional to the oscillation velocity, which was quoted and approved by Trujillo *et al.* [58]. Quadrio and Ricco [64, 65] also studied the influences of vibration parameters on drag reduction performance. Based on the results of wall oscillation velocity and period, they proposed a parameter called scaling factor and found that it was linear with drag reduction rate. Skote *et al.* [66] studied the influences of Reynolds number on the drag reduction rate when the wall oscillates in spanwise direction. They found that the maximum drag reduction rate has a power law relation with Reynolds number.

The wall oscillation velocity plays an important role in the energy balance. Baron and Quadrio [67] studied the relationship between energy saving and wall oscillation velocity for channel flow. It was found that net energy saving occured mainly when the wall oscillation velocity was relatively low. When the oscillation velocity was $U/4h$ (where U was the flow velocity in the channel and h was the half height of the channel), 10% of the net energy was saved. While, when the oscillation velocity was greater than $3U/8h$, the total energy was consumed instead of saved. It demonstrated that this drag reduction method was effective when applying oscillation with low velocity, otherwise, the external input energy consumed by creating oscillation was greater than the saved energy which was contrary to the original intention of drag reduction.

The mechanism of reducing skin friction drag based on wall oscillation can be outlined in two aspects. On one aspect, the negative spanwise vorticity can be generated by the spanwise wall oscillation, as shown in Fig.7, the mean velocity gradient in the viscous sublayer decreases and the mean velocity profile in the logarithmic layer moves up [68]. Periodic wall oscillation would cause the decrease of the streamwise vorticity associated with the longitudinal vortices. Meanwhile, negative spanwise vortices could hinder the stretching process of longitudinal vortices in the viscous sublayer, reduce the streamwise vorticity and weaken the turbulence intensity near the wall, which result in the reduction of skin friction drag [69], [70]. On another aspect, spanwise wall oscillation could interfere with the spatial correlation between near wall streamwise vortices and streak structure, leading to high-speed fluid moving away from the wall and low-speed fluid moving toward the wall which could reduce the Reynolds stress near the wall [52], [71]–[76].

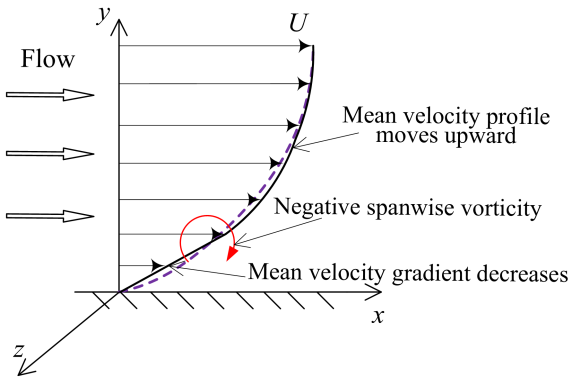

FIGURE 7. The conceptual model of turbulent boundary layer profile.

B. CREATING WALL OSCILLATION TRAVELING WAVES TO ACHIEVE DRAG REDUCTION

Zhao *et al.* [77] analyzed the drag reduction performance when wall oscillation waves propagated along the spanwise direction, as shown in Fig.5(b), a drag reduction rate of 30% was obtained. They found that new streamwise vorticities were added into the near-wall Stokes thin layer, which restrained the turbulent bursting and reduced the skin friction drag.

Quadrio and Ricco [78], [79] used DNS method to analyze the influence of the propagation characteristics of oscillation waves on the skin friction drag, as shown in Fig.5(c), and obtained the maximum drag reduction rate as 48%. They found that when the wall oscillation wave propagates along the downstream direction, the skin friction drag might increase, while when it propagates along the reverse direction, the skin friction drag always decreased. Subsequently, they also studied the effects of the propagation characteristics of the oscillation waves on the near-wall characteristics of the fluid in laminar flow [80].

Auteri *et al.* [81] studied the effect of propagation characteristics of oscillation waves on skin friction drag of turbulent pipe flow based on experiments, as shown in Fig.8, and a drag reduction rate of 33% was achieved. They found that when the wall oscillation waves propagated along the opposite direction of the flow, the skin friction drag always decreased, which was consistent with the results obtained by Quadrio et al.

Zhao *et al.* [82] analyzed the drag reduction characteristics of turbulent pipe flow when creating oscillation waves propagated on the outer wall by DNS. They found that the maximum drag reduction rate and increasing rate were both 48%. Compared with the results obtained by Quadrio et al., the maximum drag reduction rate was almost the same, while the maximum drag increasing rate increased almost by two times. They thought the reason was that the centrifugal force generated by rotation produced new

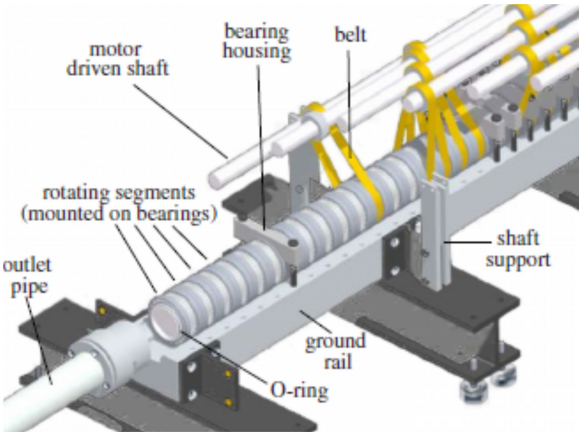

FIGURE 8. Mechanical drive of the active portion of the pipe [81].

coherent structures which increased the skin friction drag. They also found that the increase of cylindrical curvature was not conducive to drag reduction, and more net power could be saved when the amplitude decreases.

IV. DRAG REDUCTION BASED ON VOLUME FORCE CONTROL

The drag reduction method based on volume force control is to directly change the characteristics of the near wall fluid to interfere with the streak structure to achieve drag reduction. By electromagnetic actuator to generate Lorentz forces in the near wall conductive fluid or use plasma actuator to generate plasma force, the motion characteristics of the near wall fluid can be controlled. Skin friction drag reduction can be obtained by controlling the volume force oscillation wave to propagate along the spanwise direction or streamwise direction.

Well drag reduction effect can be achieved by applying spanwise oscillating volume force to the near wall fluid [83]. Berger *et al.* [84], Lee and Sung [85], Breuer *et al.* [86] and Pang and Choi [87] embedded electrodes and permanent magnets on the wall to exert spanwise oscillating electromagnetic force on the near-wall fluid to control its flow characteristics. The validity of this drag reduction method was verified based on DNS or experiments. Choi *et al.* [88] used plasma actuator to produce plasma in the near wall field and used an external electric field to control the motion characteristics of the near wall fluid. The experimental results show that this method could achieve drag reduction performance as well. Figs.9 and 10 show the details of the electromagnetic actuator and the plasma actuator, respectively.

Fuaad *et al.* [89] proposed the method of arranging heated strips along the streamwise or the spanwise direction on the wall to generate thermal buoyancy to achieve drag reduction. They found that better drag reduction performance could be obtained when the generated thermal buoyancy propagated along streamwise direction. Under this condition, the wall thermal buoyancy could interfere the distribution status of turbulent kinetic energy effectively, which formed a wide low-speed streak and restrained the velocity fluctuation.

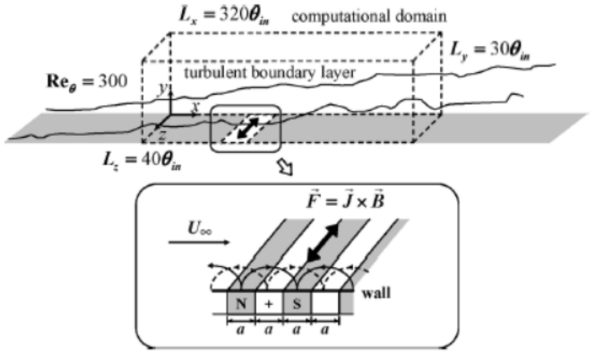

FIGURE 9. Schematic diagram of the electromagnetic actuator [85].

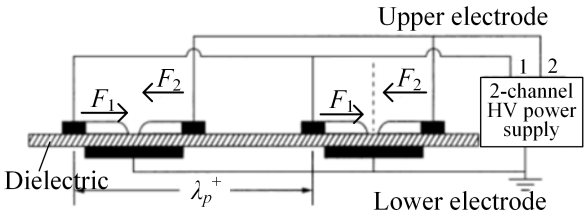

FIGURE 10. Schematic diagram of the plasma actuator [88].

In addition, they also proposed the method of combining thermal buoyancy with super-hydrophobic to achieve higher drag reduction rate [90].

Khan and Baig [91] proposed the method of controlling the near wall flow by placing monopoles / dipoles on the bottom wall of the turbulent channel to generate weak pressure disturbances, which effectively reduced the friction drag. The weak pressure disturbances reduced the occurrence of turbulent burst, weakened the turbulent kinetic energy, and reduced the friction drag.

In fact, drag reduction can be obtained whether the volume force oscillation wave propagates along the spanwise direction or along the streamwise direction.

A. CREATING SPANWISE TRAVELING WAVE TO ACHIEVE DRAG REDUCTION

Du and Karniadakis [36] used DNS to study the effect of Lorentz force oscillation waves, which were applied to near wall fluid and propagated along the spanwise direction, on turbulence suppression. The Lorentz force oscillation waves propagating along the spanwise direction could be described as:

$$f_z = Ie^{-y/\Delta} \sin(\frac{2\pi}{\lambda_z} z - \frac{2\pi}{T} t)$$

where, I was the excitation amplitude, λ_z was the spanwise wavelength, T was the period, and Δ was the penetration length. They found that this method could eliminate most of the near wall streak structures, and a drag reduction rate of 30% was achieved. Finally, they proved the validity of the DNS results by experiments. Then they studied the mechanism of reducing skin friction drag based on controlling the spanwise volume force oscillation waves [92].

They found that the volume force oscillation waves, propagating along the spanwise direction, would cause the regularization of the streamwise vorticity, and the introduction of the external streamwise vorticity would eliminate a large number of near wall streak structures. The conclusions were in agreement with the results obtained by Choi and Clayton [68].

Subsequently, Karniadakis and Choi [93] given the mechanism of the drag reduction method based on summarizing the current research results, that was, the volume force oscillation waves, which propagated along the spanwise direction, could suppress the longitudinal vortices near the wall and reduce the instability of low-speed streak structure. Schoppa and Hussain [94] also found that the longitudinal vortices could interfere with the streak structure which could achieve the drag reduction.

Fan *et al.* [95]–[98] reduced the skin friction drag by applying oscillating electromagnetic force to near-wall fluid and made the traveling wave propagate along the spanwise direction. The effect of the traveling wave on the near wall turbulent boundary layer was investigated by DNS. Xu and Choi [99] experimentally studied the characteristics of the streak structures when electromagnetic traveling waves were applied on the near wall fluid, and a drag reduction rate of 28.9% was obtained.

Choi *et al.* [88], [100] reduced the skin friction drag by driving the near wall plasma to oscillate and control the oscillation waves propagate along the spanwise direction. Through experiments, they found that the statuses of coherent structure produced by using this method were consistent with the results obtained by using electromagnetic force.

It can be seen that the skin friction drag can be reduced by applying volume force to the near wall fluid and make the generated oscillation waves propagate along the spanwise direction. The main mechanism can be described as that the oscillation waves restrain the longitudinal vortices near the wall, which weakens the instability of the streak structure near the wall and forms a wide low-speed streak.

B. CREATING STREAMWISE TRAVELING WAVE TO ACHIEVE DRAG REDUCTION

Drag reduction can also be achieved by applying oscillation volume force to the near wall fluid and make the oscillating wave propagate along the streamwise direction. Qin *et al.* [101] controlled the characteristics of turbulent boundary layer by applying oscillating Lorentz force and controlling the oscillation waves to propagate along the streamwise direction. The Lorentz force applied can be described as:

$$f_z = Ie^{-y/\Delta}\sin(\frac{2\pi}{\lambda_x}x - \frac{2\pi}{T}t)$$

where, I was the excitation amplitude, λ_x was the flow wavelength, T was the period, and Δ was the penetration length of the control force.

Based on numerical simulations, they obtained a maximum drag reduction rate of 46% and found that the drag reduction rates were different when the oscillating wave propagated along the streamwise direction and against the streamwise direction.

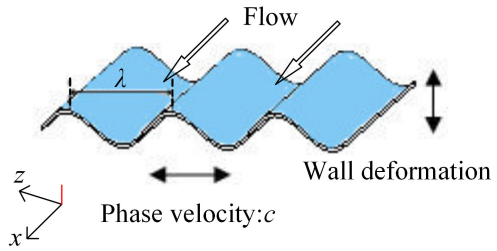

FIGURE 11. Spanwise traveling wave wall deformation.

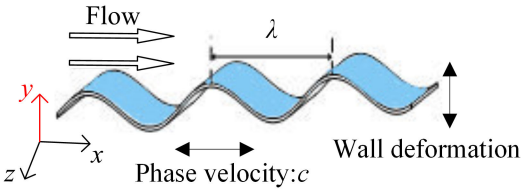

FIGURE 12. Streamwise traveling wave wall deformation.

Huang *et al.* [102] found that the drag reduction performance could be optimized by adjusting the wave number of oscillation wave, and a drag reduction rate of 42% was obtained based on the spectral analysis method. They thought that the mechanism of the drag reduction method could be described as: the propagating volume force oscillation wave along the streamwise direction induces the generalized Stokes layer to modulate the near-wall flow field. This change suppressed the frequency and intensity of turbulent bursting near the wall, which reduced the skin friction drag.

V. DRAG REDUCTION BASED ON WALL DEFORMATION

The wall deformation drag reduction method is to use external actuators to make the wall deform which could interfere with the turbulent boundary layer, so as to achieve skin friction drag reduction [103]. It can be mainly divided into: (i) spanwise traveling wave drag reduction, that is, the wall deformation generates traveling waves propagating along the spanwise direction, as shown in Fig.11; (ii) streamwise traveling wave drag reduction, that is, the wall deformation generates traveling waves propagating along the streamwise direction, as shown in Fig.12.

A. CREATING SPANWISE TRAVELING WAVE TO ACHIEVE DRAG REDUCTION

Itoh *et al.* [104] used a loudspeaker to drive the flexible plate to deform and generate spanwise traveling waves. According to the experimental results, a drag reduction rate of 7.5% was achieved. Then, they improved the driving device, as indicated in Fig.13, to optimize the drag reduction performance by adjusting the traveling wave parameters, and a drag reduction rate 13% was obtained [105].

Tomiyama and Fukagata [106] used direct numerical simulation method to study the effects of spanwise traveling

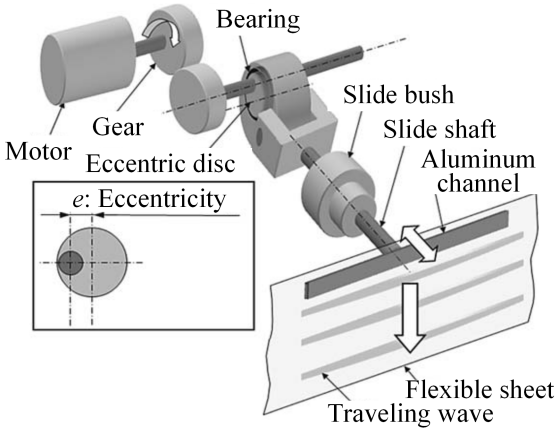

FIGURE 13. A crank excitation device [105].

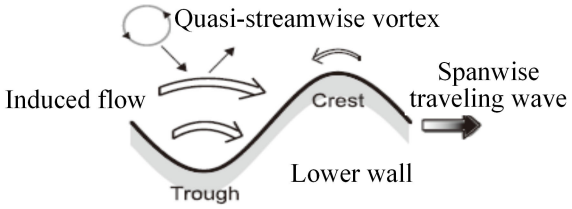

FIGURE 14. Schematic diagram of drag reduction mechanism [106].

waves, generated by wall deformation, on the characteristics of turbulent boundary layer, as shown in Fig.14. A drag reduction rate of 13.4% and a net energy saving rate of 12.2% were achieved. They thought the drag reduction mechanism of this method could be described as: the spanwise traveling waves generated by wall deformation could shield the quasi-streamwise vortices and make it away from the wall.

Klumpp *et al.* [107], [108] used a numerical method to realize drag reduction by making the wall deform and generate spanwise traveling waves, a drag reduction rate of 6% was achieved. They found that secondary flow was induced by wall deformation, which reduced the normal vorticity fluctuation of the viscous sublayer and the instability of streak structure.

Koh and Meysonnat [109]–[111] used large eddy simulation method to study the effects of Reynolds number, deformation amplitude and pressure gradient on the wall shear stress. The results shown that when the Reynolds number was relatively low, the drag reduction performance based on this method was better; with the increase of Reynolds number, the obtained drag reduction rate decreased; in a certain range, the larger the deformation amplitude, the smaller the wall shear stress; compared with the drag reduction performance in zero pressure gradient flow, the drag reduction rate in positive and negative pressure gradient flow were smaller.

Roggenkamp *et al.* [112], [113] deformed aluminum plate by using electromagnetic actuators and produced sinusoidal waves propagating along the spanwise direction, as shown in Fig.15. Based on the experimental results obtained by particle image velocimetry (PIV) and micro-particle tracking velocimetry (μ-PTV), they found that when the Reynolds number of flow field was relatively low, the higher the amplitude, the better the drag reduction performance is. A drag reduction rate of 3.4% was achieved by experiments. They thought that the mechanism could be described as: the change of turbulent boundary layer characteristics, which was caused by the traveling waves generated by wall deformation, could lead to the decrease of momentum exchange in the near wall fluid. Then, they analyzed the influences of deformation frequency and amplitude on the drag reduction performance, and obtained a maximum drag reduction rate as 4.5% [114].

Later, they proposed a method of combining passive drag reduction method (Riblet) and active drag reduction method (wall deformation drag reduction) to obtain better drag reduction performance, as shown in Fig.16 [115]. They driven aluminum plate with riblet surface to deform and generate spanwise traveling waves. Based on the PIV and μ-PTV results, they found that the drag reduction performance, when combined the two drag reduction methods, was preferable to that of taking each single drag reduction method.

It can be seen that, generating spanwise traveling waves based on wall deformation is an effective drag reduction method and combining different drag reduction method to obtain better drag reduction performance is worth further study.

B. CREATING STREAMWISE TRAVELING WAVE TO ACHIEVE DRAG REDUCTION

Taneda and Tomonari [116] proposed using cams to drive the flexible plate and generate streamwise traveling waves to reduce the skin friction drag, which was verified by experiments, as shown in Fig.17. Yao *et al.* [117] achieved a drag reduction rate of 42% by arranging several cylinders in the flow direction to drive the flexible plate to deform and generate streamwise traveling waves, as shown in Fig.18. They found that the ratio of wave velocity to flow velocity has a great influence on the separation of turbulent boundary layer and the drag reduction rate.

Shen *et al.* [118] used direct numerical simulation to analyze the influences of the velocity ratio c/U (c represents wave velocity and U represents flow velocity) on the drag reduction rate and net power saving. They found that, within a certain range ($-1.0 < c/U < 2.0$), the drag reduction rate increased with the increases of the velocity ratio, and the optimal net power saving appeared when the velocity ratio is 1.2.

Nakanishi *et al.* [119] found that when the traveling wave propagates along the positive flow direction, better drag reduction performance could be achieved. A drag reduction rate of 69% and a net energy saving rate of 65% were generated based on the DNS results.

Ahmad *et al.* [120] found that the traveling waves, generated by wall-normal velocity, propagating in the upstream direction could also effectively reduce the skin friction drag. They thought that the streamwise travelling waves of wall-normal velocity reduced the cross-flow velocity fluctuation in the buffer layer, made the velocity streak more stable,

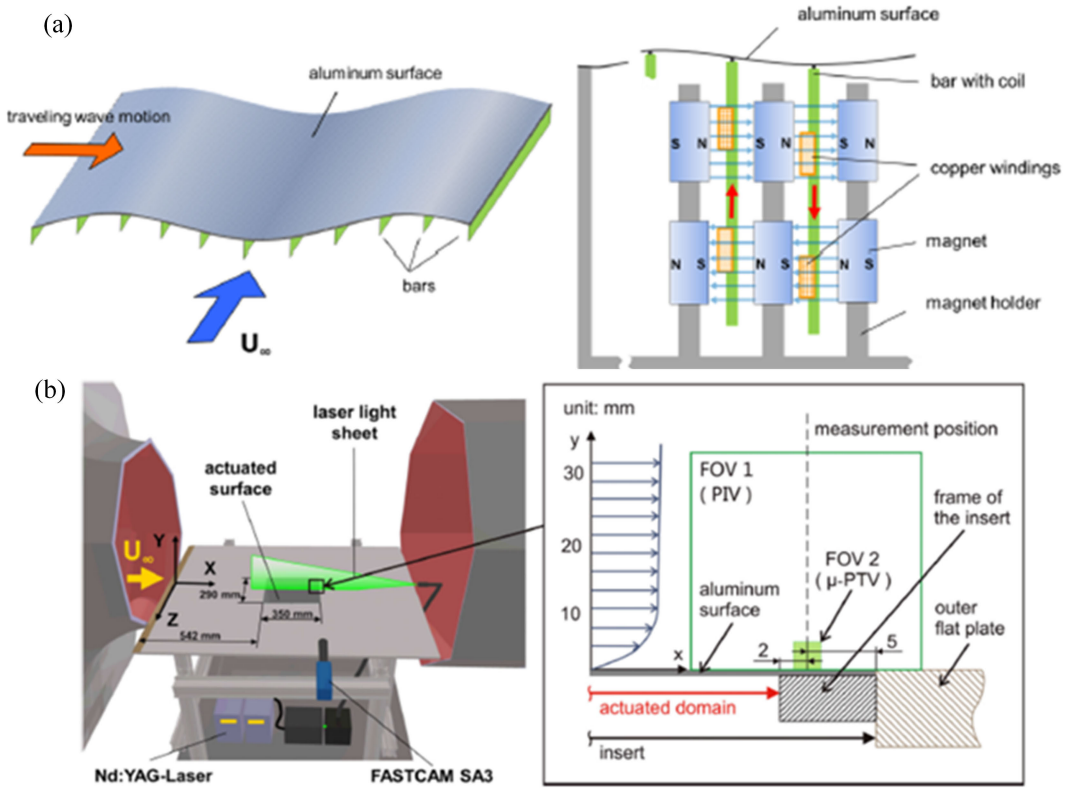

FIGURE 15. (a) Electromagnetic actuating device; (b) Schematic diagram of the experimental setup and arrangement of the PIV/μ-PTV [112].

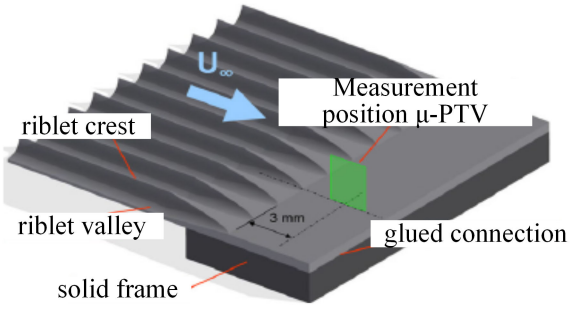

FIGURE 16. Sketch of the riblet structure and measurement position [112].

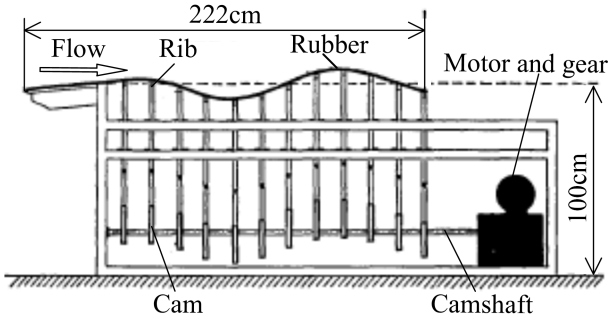

FIGURE 17. Experimental device with streamwise traveling wave wall deformation [116].

thus weakened the Reynolds shear stress and turbulent kinetic energy.

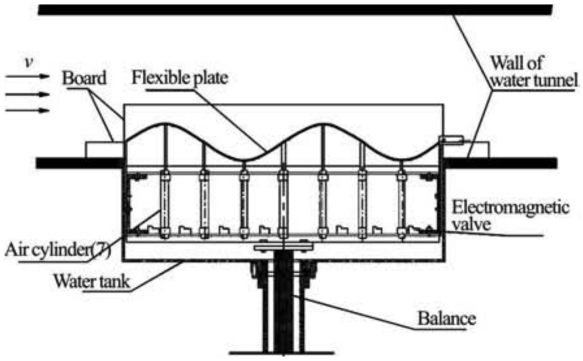

FIGURE 18. Sketch of experimental model system [117].

Mamori *et al.* [121] found through simulation analyses that the traveling wave could cause the spanwise roller-like vortices to replace the near-wall flow vortex and induce velocity slip, as shown in Fig.19. This change facilitated the generation of negative Reynolds shear stress to realize the skin friction drag reduction.

VI. DRAG REDUCTION BASED ON MICRO VIBRATION

As the turbulent boundary layer mainly exists in the near-wall fluid domain, the method of drag reduction based on micro vibration, which has the advantages of small size and fast response, has been studied [122]–[125].

The micro actuators used in drag reduction mainly include electromagnetic actuators and piezoelectric actuators,

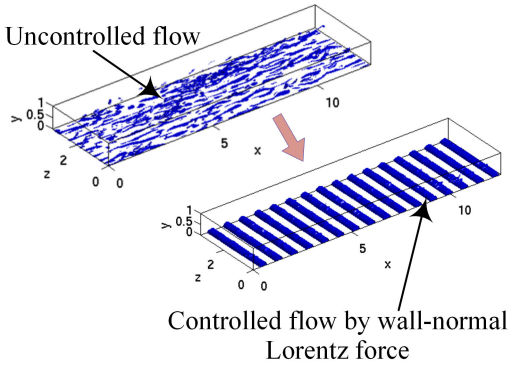

FIGURE 19. Visualization of vortexes [121].

in which the intensity of the micro vibration produced on the wall by electromagnetic actuators is larger, but it has the disadvantages of high power consumption and vulnerability to electromagnetic interference [87], [126], [127]. Piezoelectric actuators have the advantages of low power consumption, wide frequency bandwidth and immunity from electromagnetic interference. Thus, producing micro vibrations based on piezoelectric actuators is one of the hotspots in drag reduction researches [128]–[132]. Here we mainly discuss the methods of producing micro vibration on the wall by piezoelectric actuator to achieve drag reduction.

As the piezoelectric actuator could generate considerable micro vibration which could effectively control fluid when applied pulse voltages [133], it could be embedded in the wall to control turbulent coherent structure to achieve drag reduction. In 1960s, Wehrmann [134] proposed using piezoelectric ceramics to generate micro vibration on the wall to reduce the velocity fluctuation of Karman Vortex Street. Then, Wiltse and Glezer [135] modified the free shear flow characteristics in square pipes by adjusting the amplitude parameters of pulse voltages, which was applied on the piezoelectric actuators.

The main vibration parameters of piezoelectric actuator were amplitude, phase, bandwidth and frequency [136]. The relationship between amplitude and frequency, phase and frequency mainly depends on the parameters of excitation signal. While, the amplitude and bandwidth usually interact with each other, that is, to satisfy larger amplitude (bandwidth), bandwidth (amplitude) generally needs to be reduced. Therefore, in order to obtain better performance of controlling the characteristics of the boundary layer, larger vibration amplitude needs to be obtained within a given frequency range [137].

A. PIEZOELECTRIC ACTUATORS USED FOR ACHIEVING DRAG REDUCTION

1) DRAG REDUCTION BASED ON CANTILEVER PIEZOELECTRIC ACTUATOR

Cantilever piezoelectric actuator is a type of piezoelectric actuator which can provide a good balance between vibration amplitude and bandwidth for drag reduction.

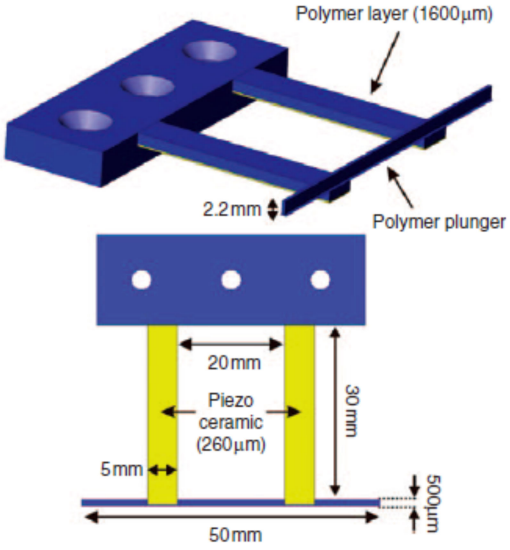

FIGURE 20. Structure sketch of PPC actuator with two cascaded single cantilever and connecting plunger [139].

Cattafesta *et al.* [138] designed a piezoelectric actuator that could achieve maximum deflection at a given bandwidth, which could cause significant flow disturbances in low-speed flow. The proportional relationships between flow velocity fluctuation, tip displacement and average velocity profile were given.

Haller *et al.* [139] designed a single cantilever piezoelectric actuator consisting of piezo-polymer-Composite (PPC) and flexible silicon film, which could form traveling waves on the wall. Then, they optimize the actuator to increase the effective propagation area of the traveling waves propagating along the spanwise direction and streamwise direction, as shown in Fig.20. They found that increasing the effective propagation area of traveling waves could obtain better drag reduction performance, that is, the piezoelectric actuators should be reasonably controlled and arranged to generate traveling waves instead of standing waves.

Mathew *et al.* [140] established finite element models, which was based on the perfect-bond theory and shear-lag theory, and analytical models of designed piezoelectric actuator. Built on the obtained results, they found that the shear-lag theory model was more accurate than the perfect-bond theory model in frequency prediction. Besides, they optimized the designed piezoelectric actuator according to the conclusions that the deformation of bimorph piezoelectric actuator was larger than that of unimorph piezoelectric actuator.

Jacobson and Reynolds [141] designed a cantilever piezoelectric actuator to reduce the skin friction drag. The experimental results proved that the micro vibration generated by piezoelectric actuator could delay the transition process of near-wall fluid from laminar to turbulent flow, and the average shear force on the downstream wall was significantly reduced. Kumar *et al.* [142] also proved that the micro vibration created by cantilever piezoelectric actuator could change the velocity profile characteristics of the near wall fluid and

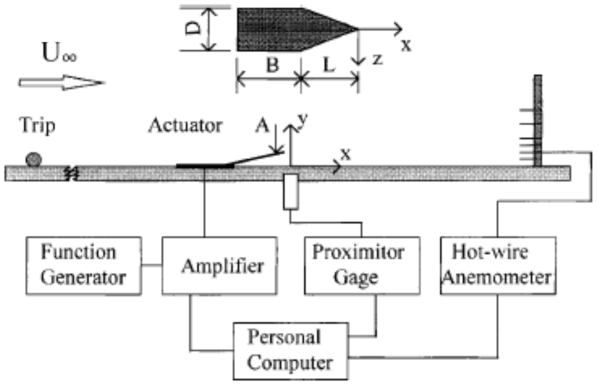

FIGURE 21. Plane view of the actuator and schematic of test equipment [145].

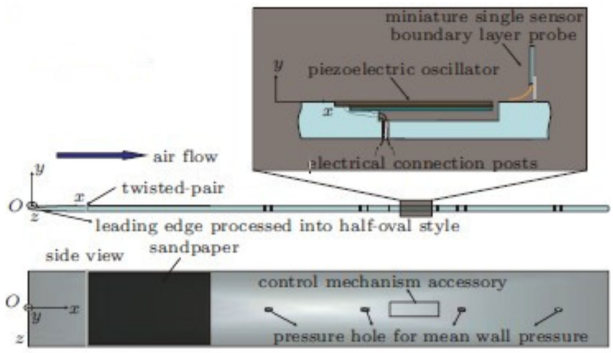

FIGURE 22. Section view of piezoelectric oscillator and schematic of experimental device [146].

reduce the skin friction drag when applied to low velocity situations.

Seifert *et al.* [143] proposed setting cantilever piezoelectric actuator on the surface of PR8-40-SE airfoil to generate micro vibration for disturbing the turbulent boundary layer and achieving wall drag reduction. They obtained the results of boundary layer velocity fluctuation, lift/drag coefficient and power efficiency under different excitation parameters.

Blackwelder *et al.* [144] designed a bimorph piezoelectric delta-wing cantilever actuator to generate wall micro vibration for drag reduction. They discovered that when the actuator was placed along downstream direction, better drag reduction effect could be achieved. Then, they analyzed the interference characteristics of micro vibration generated by the embedded unimorph piezoelectric delta-wing cantilever actuator, as shown in Fig.21, to near-wall turbulence based on experiments, which further verified the efficiency of the drag reduction method [145].

Zheng *et al.* [146] studied the interference characteristics of micro vibration generated by cantilever piezoelectric actuator on the turbulent boundary layer, based on wind tunnel experiments, as shown in Fig.22. They obtained the average flow velocity and friction stress of the near-wall fluid when the piezoelectric actuator was loaded with different voltage amplitudes and frequencies, and obtained the drag reduction

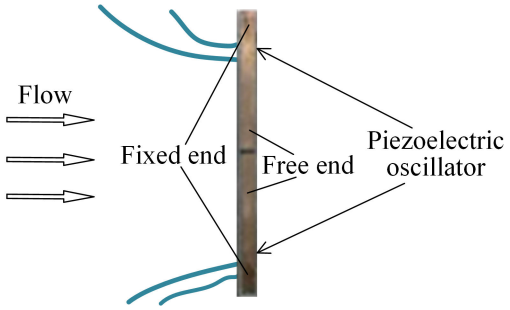

FIGURE 23. Installation schematic of two unimorph piezoelectric actuators [147].

rate with the maximum value of 26.83%. They concluded that the drag reduction performance was proportional to the vibration amplitude when the vibration frequency was constant. They thought that micro vibration of piezoelectric actuator reduced the strength of flow vortices near the wall, which decreased the skin friction drag.

Bai *et al.* [147] studied the effect of synchronous and asynchronous micro vibration created by the designed two unimorph piezoelectric cantilever actuators, as shown in Fig.23, on the near wall turbulence characteristics. Wind tunnel test results show that the drag reduction performance of asynchronous micro vibration was preferable to that of synchronous micro vibration. A drag reduction rate as 18.54% was obtained when asynchronous micro vibration was created by the two unimorph piezoelectric cantilever actuator.

Bai *et al.* [148] proposed to achieve drag reduction by placing several piezoelectric actuators on the wall and applying different excitation signals to them to generate traveling waves, as shown in Fig.24. They found that the drag reduction performance mainly was related to the wave length, vibration amplitude and vibration frequency. Based on the wind tunnel test results, a local drag reduction rate of up to 50% was achieved. They thought that the mechanism could be explained as follows: the traveling waves produced a regularized streamwise vorticity, which hindered the interaction effect between the near wall fluid and the large-scale turbulent structure, and suppressed the turbulent bursting. Then, they studied the changes of streak structure under micro vibration, and found that the traveling waves, generated by micro vibration created by piezoelectric actuator, made the streak structure orderly and reduced the turbulent kinetic energy [149].

2) DRAG REDUCTION BASED ON BONDED PIEZOELECTRIC PLATE

Mansoor *et al.* [150] proposed the use of bonded piezoelectric plate to generate micro vibration on the wing surface to achieve drag reduction, and studied its non-linear characteristics. Then, they designed a small bounded type non-linear rectangular actuator to achieve wall drag reduction, as shown in Fig.25. The vibration with amplitude as 250 μm was

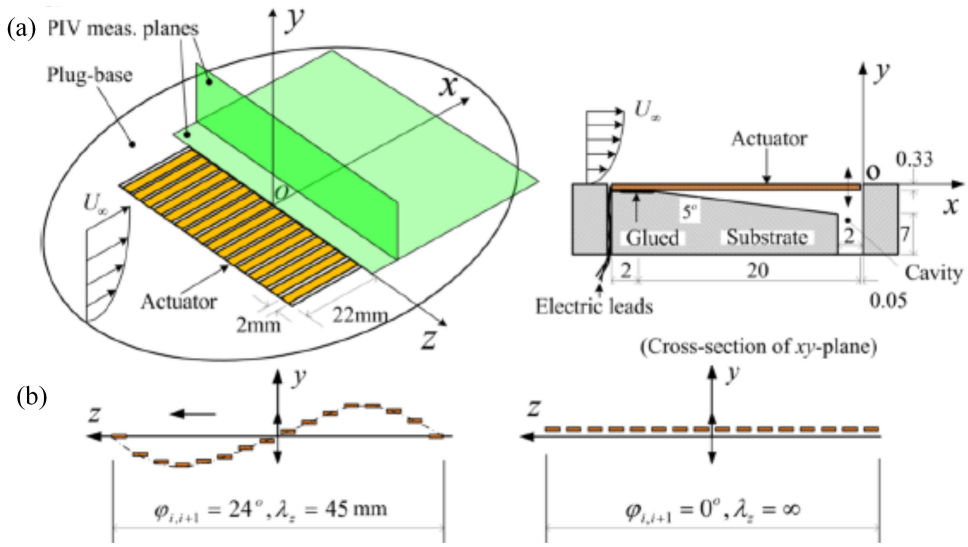

FIGURE 24. (a) Layout schematic of the 16 piezoelectric actuators; (b) Spanwise wave formed at $\varphi_{i,i+1} = 24°$ and $\varphi_{i,i+1} = 0°$ [149].

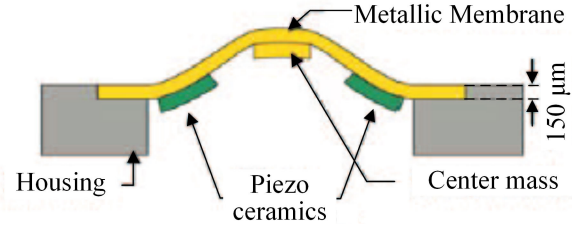

FIGURE 25. Cross sectional view of rectangular actuator [151].

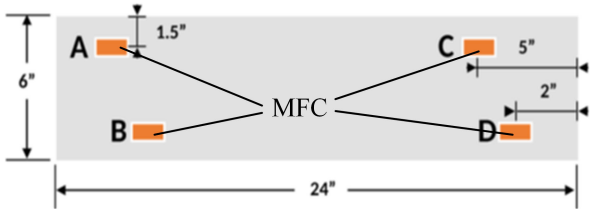

FIGURE 27. Locations of four MFCs bounded on the plate [154].

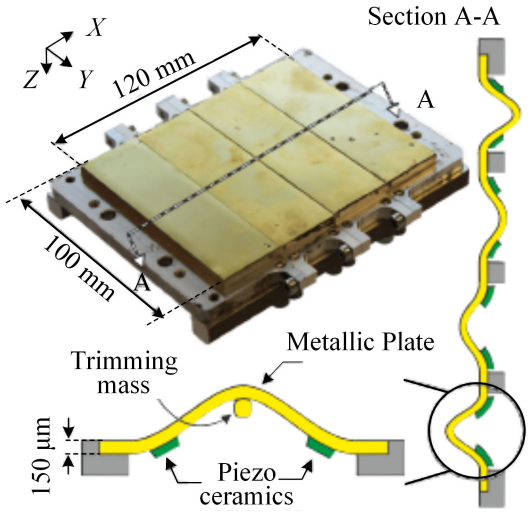

FIGURE 26. Structural schematic diagram of four cascaded actuator [152].

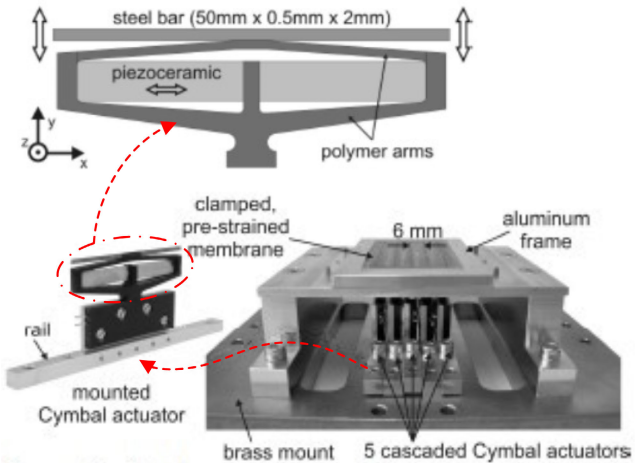

FIGURE 28. Structural schematic diagram of five cascaded cymbal actuators connected to a brass mount [157].

obtained in an effective frequency range. They found that the frequency response fluctuation could be eliminated by pasting a center mass on the metallic membrane [151]. Subsequently, they designed a non-linear actuator consisting of four piezoelectric ceramic arrays and metallic plate, which could generate large amplitude traveling waves on the wall to achieve drag reduction, as shown in Fig.26. They optimized the thickness and the spacing of piezoelectric ceramics to reduce the bending stress of piezoelectric ceramics when the maximum amplitude was obtained [152].

Malladi *et al.* [153] used two Macro-Fiber Composite (MFC) piezoelectric actuators to generate micro vibration on a flat plate to achieve wall drag reduction. Then, they studied the influence of the arrangement and excitation of MFC actuators on the formation characteristics

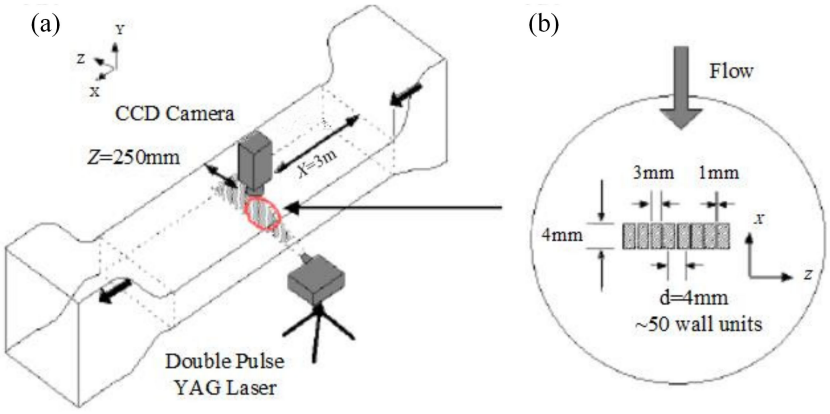

FIGURE 29. (a) Water channel system and the placement of PIV; (b) Eight piezoelectric actuators arranged along the spanwise direction [158].

of traveling wave, which was beneficial to achieve drag reduction [154]. They analyzed the vibration results of four MFC piezoelectric actuators under different loading modes (excite A and B, excite A and C, excite A and D), as shown in Fig.27. They found that when only exciting A-B or A-C, standing waves could be formed on the plate, while when exciting A-D, traveling waves could be formed on the plate.

In order to reduce the wall drag of ship-like hull, we proposed to bond piezoelectric ceramics on the inner wall to generate micro vibration. The effects of related parameters on the drag reduction performance were obtained by simulations and experiments [155].

3) DRAG REDUCTION BASED ON PIEZOELECTRIC COMPOSITE ACTUATOR

Papila *et al.* [156] optimized a clamped circular piezoelectric ceramic actuator for flow control. In the given design range, the optimum thickness and radius of piezoelectric sheet were obtained by analytic solutions. They concluded that a power law relationship exists between displacement and bandwidth, that is, the gain–bandwidth product was constant.

In order to reduce the space occupied by the piezoelectric actuators, Haller *et al.* [157] designed cymbal piezoelectric polymer composite actuators, as shown in Fig.28. Based on the wind experimental results, it was proved that the micro vibration generated by the actuator could effectively reduce the instability of fluid flow on the wing surface and achieve well drag reduction performance.

Segawa *et al.* [158] placed several piezoelectric ceramic actuators on the outer wall of the water channel to generate traveling waves to achieve drag reduction, as shown in Fig.29. The drag reduction performance was tested by PIV experiments. They thought that the main reason for achieving drag reduction was that the traveling waves corrected the near wall longitudinal vortices and suppressed the coherent structure near the wall.

B. CONTROL METHODS OF PIEZOELECTRIC ACTUATOR FOR DRAG REDUCTION

The control methods of piezoelectric actuator used for drag reduction mainly include open-loop control methods and closed-loop control methods. For closed-loop control method, the information of wall shear stress, wall pressure, and flow velocity was obtained by sensors and be fed back to the control system, so as to adjust the working state of piezoelectric actuator to obtain stable drag reduction performance [159]–[162]. Compared with open-loop control, closed-loop control could achieve better drag reduction performance, because turbulent boundary layer has the characteristics of randomness and spatio-temporal intermittence [163]–[166]. Kasagi *et al.* [167], Zhou and Bai [168] and Brunton and Noack [169] summarized the state of art of achieving active drag reduction based on closed-loop control methods. It could be seen that for drag reduction based on closed-loop control, experiments were difficult to be carried out. The main reason was that the information of the turbulent boundary layer was hard to be obtained in time and accurately by a small number of sensors.

Jacobson and Reynolds [141] used piezoelectric actuators to produce steady and unsteady disturbances in the boundary layer built on closed-loop control, which reduced the shear stress on the downstream wall.

The drag reduction method based on piezoelectric micro vibration proposed by Bai *et al.* [148] obtained well drag reduction performance, but the control efficiency was relatively low. Thus, Zhou *et al.* [170] placed sensors in the upstream and downstream areas of piezoelectric actuators to measure wall shear force, so as to achieve piezoelectric vibration drag reduction based on closed-loop control, as shown in Fig.30. They compared the performance of piezoelectric vibration drag reduction under different control methods, and concluded that closed-loop control could save a lot of energy. Then, they studied the drag reduction performance under different closed-loop control methods, and verified the results through wind tunnel experiments [171].

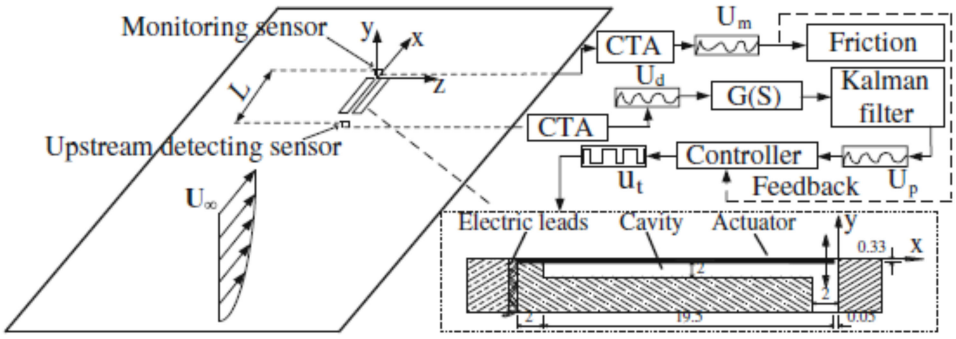

FIGURE 30. Schematic of experimental arrangement [170].

TABLE 1. Drag reduction performance based on wall motion.

Reference	Action mode	Research method	Drag reduction rate	Conditions
Viotti et al. [51]	Wall oscillation	Simulation	52%	$A^+ = 20$, $\lambda_x^+ = 1250$
Jung et al. [55, 56]		Simulation	10% ~ 40%	$25 \le T^+ \le 200$
Laadhari et al. [57]		Experiment	45%	$0.0033 \le f^+ \le 0.0166$
Trujillo et al. [58]		Experiment	25%	—
Choi et al. [59]		Experiment	25%	$50 \le T^+ \le 100$
Quadrio et al. [60]		Simulation	40%	—
Choi et al. [63, 68]		Experiment	45%	—
Quadrio et al. [64]		Simulation	44.7%	$T^+ = 100$
Baron et al. [67]		Simulation	40%	—
Miyake et al. [69]		Simulation	35%	$T^+ = 100$
Cicca et al. [75]		Experiment	25%	$T^+ = 100$, $\Delta z^+ = 324$
Zhao et al. [77]	Oscillation traveling waves	Simulation	30%	$T^+ = 50$, $\lambda^+ = 2\pi$
Quadrio et al. [78, 79]		Simulation	48%	$A^+ = 12$, $Re = 4760$
Auteri et al. [81]		Experiment	33%	—
Zhao et al. [82]		Simulation	48%	$A^+ = 16$, $\omega^+ = 0.0126$, $k_x^+ = 0.0148$

VII. DISCUSSIONS AND CONCLUSION

The skin friction force is mainly created due to the coherent structure which exists in turbulent boundary layer. Active interference of the coherent structure of turbulent boundary layer can restrain the turbulent bursting and reduce the skin friction force effectively. In this work, based on the actuation mode, we divide the active drag reduction methods as: drag reduction based on wall motion, drag reduction based on volume force control, drag reduction based on wall deformation and drag reduction based on micro vibration. The states of the art of each active drag reduction method are discussed and conclusions are summarized:

1) According to the motion form, drag reduction based on wall motion can be divided into drag reduction based on spanwise wall oscillation and drag reduction based on oscillation traveling waves. The spanwise wall oscillation could interfere with the spatial correlation between near wall streamwise vortices and streak structure, leading to high-speed fluid moving away from the wall and low-speed fluid moving toward the wall which could achieve the drag reduction. The oscillation traveling waves could create new streamwise vorticities in the turbulent boundary layer, which restrained the turbulent bursting and reduced the skin friction drag. The drag reduction performance is listed in Table 1. Quantities with the "+" superscript in the Table 1 are made dimensionless with viscous wall units, which are also applicable to the following table. The drag reduction method based on wall motion is suitable for plates and pipes which can accept oscillating motion, such as the walls of oil / natural gas transportation pipeline, swept wing of aircraft, etc.

2) The drag reduction method based on volume force control is that applying electrodes and permanent magnets to generate Lorentz forces in the near wall conductive fluid or apply plasma actuator to generate plasma force, and induce the generation of traveling waves. Based on the propagate direction, it can be divided into drag reduction based on spanwise traveling waves and streamwise traveling waves. The traveling waves, propagating along spanwise direction, could suppress the longitudinal vortices near the wall and reduce the instability of low-speed streak structure, which can achieve the drag reduction. The traveling waves, propagating along streamwise direction, could suppress the frequency and intensity of turbulent bursting near the wall, which reduced the skin friction drag. The drag reduction performance is in Table 2. The drag reduction method based on volume force control is suitable for the situations where the target wall moves in conductive fluid or plasma could be generated in the

TABLE 2. Drag reduction performance based on volume force control.

Reference	Action mode	Research method	Drag reduction rate	Conditions
Berger et al. [84]	Spanwise oscillating volume force	Simulation	40%	$Re_\tau = 100$
Lee et al. [85]		Simulation	20%	$T^+ = 100$
Breuer et al. [86]		Experiment	10%	$T^+ = 100$
Pang et al. [87]		Experiment	40%	St = 210, $T^+ = 100$
Choi et al. [88]		Experiment	45%	—
Du et al. [36]	Spanwise traveling waves volume force	Simulation	30%	I =1, $T^+ = 50$, $\lambda_z{}^+ = 840$
Du et al. [92]		Experiment	35%	$T^+ = 100$
Fan et al. [98]		Simulation	30%	$T^+ = 40$, $k_z = 1$, $\lambda_z{}^+ = 377$
Qin et al. [101]	Streamwise traveling waves volume force	Simulation	46%	$T^+ = 100$, $\lambda_x = \pi$
Huang et al. [102]		Simulation	42%	$\lambda_x{}^+ = 188$, $T = 8$

TABLE 3. Drag reduction performance based on wall deformation.

Reference	Action mode	Research method	Drag reduction rate	Conditions
Itoh et al. [104]	Spanwise traveling waves wall deformation	Experiment	7.5%	$A^+ = 16$, $f^+ = 0.010$
Tamano et al. [105]		Experiment	13%	$T^+ = 115$, $A_{avc}{}^+ = 24$
Tomiyama et al. [106]		Simulation	13.4%	$T^+ = 181$, $\lambda_z{}^+ = 141$
Klumpp et al. [107, 108]		Simulation	6%	$T^+ = 50$, $\lambda_z{}^+ = 870$
Koh et al. [109]		Simulation	11%	$Re_\theta = 1000$
Meysonnat et al. [110, 111]		Simulation	11.4%	$A^+ = 50$, $Re_\theta = 2000$
Roggenkamp et al. [112]		Experiment	3.4%	$A^+ = 9$, $Re_\theta = 1200$
Li et al. [114]		Experiment	4.5%	$A^+ = 11.8$, $T^+ = 110$
Li et al. [112]		Experiment	9.4%	$A^+ = 9$, $Re_\theta = 1200$, $T^+ = 110$
Yao et al. [117]	Streamwise traveling waves wall deformation	Experiment	42%	$c/U = 1.26$
Nakanishi et al. [119]		Simulation	69%	—
Mamori et al. [121]		Simulation	23%	—

TABLE 4. Drag reduction performance based on wall micro vibration.

Reference	Action mode	Control method	Drag reduction rate	Conditions
Zheng et al. [146]	Micro vibration based on piezoelectric actuators	—	26.83%	100V, 160Hz
Bai et al. [147]		Synchronous and asynchronous vibration	18.54%	100V, 160Hz, asynchronous vibration
Bai et al. [148]		Open-loop	50%	$A^+ = 2$, $f^+ > 0.39$, $\lambda_z{}^+ = 250$, $x^+ = 17$
Zhou et al. [170, 171]		Open-loop / feed-forward / combined feed-forward and feedback control	30% / 24% / 29%	$A^+ = 1.61$, $f^+ = 0.56$, $x^+ = 14$

near wall, such as the walls of underwater vehicle, high-speed train, aircraft wing wall, etc.

3) The drag reduction method based on wall deformation is to make the wall deform by external actuators to create traveling waves on the wall, which could interfere with the turbulent boundary layer and reduce the skin friction force. The traveling waves could change the characteristics of the turbulent boundary layer and reduce the momentum exchange in the near wall fluid, which can achieve the drag reduction. Based on the propagate direction, the method also can be divided into drag reduction based on spanwise traveling waves and drag reduction based on streamwise traveling waves. The drag reduction performance is listed in Table 3. This drag reduction is suitable for flexible walls that can deform, such as the walls of flexible vehicle, flexible aircraft, etc.

4) For drag reduction based on micro vibration, which is mainly produced by piezoelectric actuator, although the driven deformation amplitude is small, the vibration velocity of the micro vibration is large enough to interfere with the turbulent boundary layer. The piezoelectric actuators, used for producing micro vibration, mainly are cantilever piezoelectric actuator, bonded piezoelectric plate and piezoelectric composite actuator. Methods for controlling the piezoelectric actuators mainly include open-loop control methods and closed-loop control methods. Closed-loop control methods could obtain better drag reduction performance than open-loop control methods, while the control systems are more complicated and costly. The drag reduction performance is listed in Table 4. By controlling the micro vibration to form traveling waves also could obtain better drag reduction performance, the traveling waves could produce

regularized streamwise vorticities, which hindered the large-scale turbulent structure and suppressed the turbulent bursting. This method is suitable for general walls that can withstand relatively high frequency vibrations, such as the walls of underwater vehicle, aircraft wing, rocket, etc.

5) Besides, it can be seen that, achieving drag reduction by traveling waves is more effective and the drag reduction performance can be adjusted by controlling the characteristics of the traveling waves. It is also a trend to combine active control method with passive control method to achieve better drag reduction performance.

REFERENCES

[1] J. L. Lumley, "Flow control: Passive, active and reactive flow management," *SIAM Rev.*, vol. 43, no. 4, pp. 726–727, 2000.
[2] A. Abbas, G. Bugeda, E. Ferrer, S. Fu, J. Periaux, J. Pons-Prats, E. Valero, and Y. Zheng, "Drag reduction via turbulent boundary layer flow control," *Sci. China-Technol. Sci.*, vol. 60, pp. 1281–1290, Sep. 2017.
[3] M. Gad-el-Hak, "Flow control: The future," *J. Aircr.*, vol. 38, no. 3, pp. 402–418, May 2001.
[4] L. Lofdahl and M. Gad-el-Hak, "MEMS applications in turbulence and flow control," *Prog. Aerosp. Sci.*, vol. 35, no. 2, pp. 101–203, Feb. 1999.
[5] D. M. Bushnell, "Aircraft drag reduction—A review," *Proc. Inst. Mech. Eng. G, J. Aerosp. Eng.*, vol. 217, pp. 1–18, Jan. 2003.
[6] R. Rathnasingham and K. S. Breuer, "System identification and control of a turbulent boundary layer," *Phys. Fluids*, vol. 9, no. 7, pp. 1867–1869, Jul. 1997.
[7] R. Rathnasingham and K. S. Breuer, "Active control of turbulent boundary layers," *J. Fluid Mech.*, vol. 495, pp. 209–233, Nov. 2003.
[8] M. Gad-el-Hak and D. M. Bushnell, "Separation control: Review," *J. Fluids Eng.-Trans. ASME*, vol. 113, pp. 5–30, Mar. 1991.
[9] M. Alrefai and M. Acharya, "Controlled leading-edge suction for management of unsteady separation over pitching airfoils," *AIAA J.*, vol. 34, no. 11, pp. 2327–2336, Nov. 1996.
[10] C. Warsop, M. Hucker, A. J. Press, and P. Dawson, "Pulsed air-jet actuators for flow separation control," *Flow Turbulence Combustion*, vol. 78, pp. 255–281, Jun. 2007.
[11] N. Tounsi, R. Mestiri, L. Keirsbulck, H. Oualli, S. Hanchi, and F. Aloui, "Experimental study of flow control on bluff body using piezoelectric actuators," *JAFM*, vol. 9, no. 2, pp. 827–838, Mar. 2016.
[12] M. Gad-el-Hak, "Modern developments in flow control," *Appl. Mech. Rev.*, vol. 49, no. 7, pp. 365–379, Jul. 1996.
[13] E. Moreau, "Airflow control by non-thermal plasma actuators," *J. Phys. D, Appl. Phys.*, vol. 40, no. 3, pp. 605–636, Feb. 2007.
[14] F. Lundell, "Reactive control of transition induced by free-stream turbulence: An experimental demonstration," *J. Fluid Mech.*, vol. 585, pp. 41–71, Aug. 2007.
[15] F. Xu, W.-L. Chen, W.-F. Bai, Y.-Q. Xiao, and J.-P. Ou, "Flow control of the wake vortex street of a circular cylinder by using a traveling wave wall at low Reynolds number," *Comput. Fluids*, vol. 145, pp. 52–67, Mar. 2017.
[16] F. Xu, W.-L. Chen, Y.-Q. Xiao, H. Li, and J.-P. Ou, "Numerical study on the suppression of the vortex-induced vibration of an elastically mounted cylinder by a traveling wave wall," *J. Fluids Struct.*, vol. 44, pp. 145–165, Jan. 2014.
[17] D. M. Bushnell and C. B. McGinley, "Turbulence control in wall flows," *Annu. Rev. Fluid Mech.*, vol. 21, pp. 1–20, Jan. 1989.
[18] J. Lumley and P. Blossey, "Control of turbulence," *Annu. Rev. Fluid Mech.*, vol. 30, pp. 311–327, Jan. 1998.
[19] E. J. Gutmark, K. C. Schadow, and K. H. Yu, "Mixing enhancement in superaonic free shear flows," *Annu. Rev. Fluid Mech.*, vol. 27, pp. 375–417, Jan. 1995.
[20] T. C. Corke and F. O. Thomas, "Active and passive turbulent boundary–layer drag reduction," *AIAA J.*, vol. 56, no. 10, pp. 3835–3847, Oct. 2018.
[21] G. Yunqing, L. Tao, M. Jiegang, S. Zhengzan, and Z. Peijian, "Analysis of drag reduction methods and mechanisms of turbulent," *Appl. Bionics Biomech.*, vol. 2017, pp. 1–8, Sep. 2017.
[22] B.-Q. Deng, W.-X. Huang, and C.-X. Xu, "Origin of effectiveness degradation in active drag reduction control of turbulent channel flow at Re=1000," *J. Turbulence*, vol. 17, no. 8, pp. 758–786, Aug. 2016.
[23] M. Xiang, H. Zhou, and W. Yang, "Unsteady dynamic analysis for the cavitating hydrofoils based on OpenFOAM," *Exp. Comput. Multiph. Flow*, vol. 1, no. 2, pp. 101–108, Jun. 2019.
[24] J. Jiménez, J. C. Del Alamo, and O. Flores, "The large-scale dynamics of near-wall turbulence," *J. Fluid Mech.*, vol. 505, pp. 179–199, Apr. 2004.
[25] K. Iwamoto, K. Fukagata, N. Kasagi, and Y. Suzuki, "Friction drag reduction achievable by near-wall turbulence manipulation at high Reynolds numbers," *Phys. Fluids*, vol. 17, no. 1, pp. 011702-1–011702-4, Jan. 2005.
[26] J. Jiménez and A. Pinelli, "The autonomous cycle of near-wall turbulence," *J. Fluid Mech.*, vol. 389, pp. 335–359, Jun. 1999.
[27] J. C. R. Hunt and J. F. Morrison, "Eddy structure in turbulent boundary layers," *Eur. J. Mech. B-Fluids*, vol. 19, pp. 673–694, Sep./Oct. 2000.
[28] K. T. Christensen and R. J. Adrian, "Statistical evidence of hairpin vortex packets in wall turbulence," *J. Fluid Mech.*, vol. 431, pp. 433–443, Mar. 2001.
[29] J. Zhou, R. J. Adrian, S. Balachandar, and T. M. Kendall, "Mechanisms for generating coherent packets of hairpin vortices in channel flow," *J. Fluid Mech.*, vol. 387, pp. 353–396, May 1999.
[30] P. S. Klebanoff, "Characteristics of turbulence in a boundary layer with zero pressure gradient," NACA, Washington, DC, USA, Tech. Note 1247, Jan. 1954.
[31] S. J. Kline and S. K. Robinson, "Quasi-coherent structures in the turbulent boundary-layer. 1. Status-report on a community-wide summary of the data," in *Proc. Near-Wall Turbulence Zoran Zaric Memorial Conf.*, vol. 28, 1990, pp. 200–217.
[32] S. S. Lu and W. W. Willmarth, "Measurements of the structure of the Reynolds stress in a turbulent boundary layer," *J. Fluid Mech.*, vol. 60, no. 03, p. 481, Sep. 1973.
[33] S. K. Robinson, "Coherent motions in the turbulent boundary-layer," *Annu. Rev. Fluid Mech.*, vol. 23, pp. 601–639, Jan. 1991.
[34] N. Aubry, P. Holmes, J. L. Lumley, and E. Stone, "The dynamics of coherent structures in the wall region of a turbulent boundary layer," *J. Fluid Mech.*, vol. 192, pp. 115–173, Jul. 1988.
[35] A. V. Johansson, P. H. Alfredsson, and J. Kim, "Evolution and dynamics of shear-layer structures in near-wall turbulence," *J. Fluid Mech.*, vol. 224, pp. 579–599, Mar. 1991.
[36] Y. Du, "Suppressing wall turbulence by means of a transverse traveling wave," *Science*, vol. 288, no. 5469, pp. 1230–1234, May 2000.
[37] J. Jeong, F. Hussain, W. Schoppa, and J. Kim, "Coherent structures near the wall in a turbulent channel flow," *J. Fluid Mech.*, vol. 332, pp. 185–214, Feb. 1997.
[38] R. L. Panton, "Overview of the self-sustaining mechanisms of wall turbulence," *Prog. Aerosp. Sci.*, vol. 37, no. 4, pp. 341–383, May 2001.
[39] F. Waleffe, "On a self-sustaining process in shear flows," *Phys. Fluids*, vol. 9, no. 4, pp. 883–900, Apr. 1997.
[40] W. Schoppa and F. Hussain, "Coherent structure dynamics in near-wall turbulence," *Fluid Dyn. Res.*, vol. 26, no. 2, pp. 119–139, Feb. 2000.
[41] D. K. Heist, T. J. Hanratty, and Y. Na, "Observations of the formation of streamwise vortices by rotation of arch vortices," *Phys. Fluids*, vol. 12, no. 11, p. 2965, 2000.
[42] P. S. Bernard, J. M. Thomas, and R. A. Handler, "Vortex dynamics and the production of Reynolds stress," *J. Fluid Mech.*, vol. 253, pp. 385–419, Aug. 1993.
[43] M. Asai, M. Minagawa, and M. Nishioka, "The instability and breakdown of a near-wall low-speed streak," *J. Fluid Mech.*, vol. 455, pp. 289–314, Mar. 2002.
[44] J. M. Hamilton, J. Kim, and F. Waleffe, "Regeneration mechanisms of near-wall turbulence structures," *J. Fluid Mech.*, vol. 287, pp. 317–348, Mar. 1995.
[45] W. Schoppa and F. Hussain, "Coherent structure generation in near-wall turbulence," *J. Fluid Mech.*, vol. 453, pp. 57–108, Feb. 2002.
[46] B.-Q. Deng and C.-X. Xu, "Influence of active control on STG-based generation of streamwise vortices in near-wall turbulence," *J. Fluid Mech.*, vol. 710, pp. 234–259, Nov. 2012.
[47] T. Endo, N. Kasagi, and Y. Suzuki, "Feedback control of wall turbulence with wall deformation," *Int. J. Heat Fluid Flow*, vol. 21, no. 5, pp. 568–575, Oct. 2000.
[48] A. G. Kravchenko, H. Choi, and P. Moin, "On the relation of near-wall streamwise vortices to wall skin friction in turbulent boundary layers," *Phys. Fluids A, Fluid Dyn.*, vol. 5, no. 12, pp. 3307–3309, Dec. 1993.
[49] J. H. Kim and J. H. Lee, "Skin-friction drag reduction in turbulent channel flow based on streamwise shear control," *Int. J. Heat Fluid Flow*, vol. 63, pp. 28–43, Feb. 2017.

[50] A. Yakeno, Y. Hasegawa, and N. Kasagi, "Modification of quasi-streamwise vortical structure in a drag-reduced turbulent channel flow with spanwise wall oscillation," *Phys. Fluids*, vol. 26, no. 8, Aug. 2014, Art. no. 085109.

[51] C. Viotti, M. Quadrio, and P. Luchini, "Streamwise oscillation of spanwise velocity at the wall of a channel for turbulent drag reduction," *Phys. Fluids*, vol. 21, no. 11, Nov. 2009, Art. no. 115109.

[52] E. Touber and M. A. Leschziner, "Near-wall streak modification by spanwise oscillatory wall motion and drag-reduction mechanisms," *J. Fluid Mech.*, vol. 693, pp. 150–200, Feb. 2012.

[53] C. A. Duque-Daza, M. F. Baig, D. A. Lockerby, S. I. Chernyshenko, and C. Davies, "Modelling turbulent skin-friction control using linearized Navier-Stokes equations," *J. Fluid Mech.*, vol. 702, pp. 403–414, Jul. 2012.

[54] P. Bradshaw and N. S. Pontikos, "Measurements in the turbulent boundary-layer on an infinite swept wing," *J. Fluid Mech.*, vol. 159, pp. 105–130, Oct. 1985.

[55] W. J. Jung, N. Mangiavacchi, and R. Akhavan, "Suppression of turbulence in wall-bounded flows by high-frequency spanwise oscillations," *Phys. Fluids A, Fluid Dyn.*, vol. 4, no. 8, pp. 1605–1607, Aug. 1992.

[56] R. Akhavan, W. J. Jung, and N. Mangiavacchi, "Turbulence control in wall-bounded flows by spanwise oscillations," *Appl. Sci. Res.*, vol. 51, pp. 299–303, Jun. 1993.

[57] F. Laadhari, L. Skandaji, and R. Morel, "Turbulence reduction in a boundary layer by a local spanwise oscillating surface," *Phys. Fluids*, vol. 6, no. 10, pp. 3218–3220, Oct. 1994.

[58] S. Trujillo, D. Bogard, K. Ball, S. Trujillo, D. Bogard, and K. Ball, "Turbulent boundary layer drag reduction using an oscillating wall," in *Proc. 4th Shear Flow Control Conf.*, Snowmass Village, CO, USA, Jun. 1997.

[59] K.-S. Choi and M. Graham, "Drag reduction of turbulent pipe flows by circular-wall oscillation," *Phys. Fluids*, vol. 10, no. 1, pp. 7–9, Jan. 1998.

[60] M. Quadrio and S. Sibilla, "Numerical simulation of turbulent flow in a pipe oscillating around its axis," *J. Fluid Mech.*, vol. 424, pp. 217–241, Dec. 2000.

[61] A. Duggleby, K. S. Ball, and M. R. Paul, "The effect of spanwise wall oscillation on turbulent pipe flow structures resulting in drag reduction," *Phys. Fluids*, vol. 19, no. 12, Dec. 2007, Art. no. 125107.

[62] M. S. Naim and M. F. Baig, "Turbulent drag reduction in Taylor–Couette flows using different super-hydrophobic surface configurations," *Phys. Fluids*, vol. 31, no. 9, Sep. 2019, Art. no. 095108.

[63] K.-S. Choi, J.-R. Debisschop, and B. R. Clayton, "Turbulent boundary-layer control by means of spanwise-wall oscillation," *AIAA J.*, vol. 36, pp. 1157–1163, Jan. 1998.

[64] M. Quadrio and P. Ricco, "Critical assessment of turbulent drag reduction through spanwise wall oscillations," *J. Fluid Mech.*, vol. 521, pp. 251–271, Dec. 2004.

[65] P. Ricco and M. Quadrio, "Wall-oscillation conditions for drag reduction in turbulent channel flow," *Int. J. Heat Fluid Flow*, vol. 29, no. 4, pp. 891–902, Aug. 2008.

[66] M. Skote, M. Mishra, and Y. Wu, "Drag reduction of a turbulent boundary layer over an oscillating wall and its variation with Reynolds number," *Int. J. Aerosp. Eng.*, vol. 2015, pp. 1–9, Nov. 2015.

[67] A. Baron and M. Quadrio, "Turbulent drag reduction by spanwise wall oscillations," *Appl. Sci. Res.*, vol. 55, no. 4, pp. 311–326, 1996.

[68] K.-S. Choi and B. R. Clayton, "The mechanism of turbulent drag reduction with wall oscillation," *Int. J. Heat Fluid Flow*, vol. 22, no. 1, pp. 1–9, Feb. 2001.

[69] Y. Miyake, K. Tsujimoto, and M. Takahashi, "On the mechanism of drag reduction of near-wall turbulence by wall oscillation," *JSME Int. J.*, vol. 40, pp. 558–566, Nov. 1997.

[70] K.-S. Choi, "Near-wall structure of turbulent boundary layer with spanwise-wall oscillation," *Phys. Fluids*, vol. 14, no. 7, pp. 2530–2542, 2002.

[71] M. R. Dhanak and C. Si, "On reduction of turbulent wall friction through spanwise wall oscillations," *J. Fluid Mech.*, vol. 383, pp. 175–195, Mar. 1999.

[72] G. Iuso, G. M. Di Cicca, M. Onorato, P. G. Spazzini, and R. Malvano, "Velocity streak structure modifications induced by flow manipulation," *Phys. Fluids*, vol. 15, no. 9, pp. 2602–2612, Sep. 2003.

[73] J. K. Eaton, "Effects of mean flow 3-dimensionality on turbulent boundary-layer structure," *AIAA J.*, vol. 33, pp. 2020–2025, Nov. 1995.

[74] P. Ricco, "Modification of near-wall turbulence due to spanwise wall oscillations," *J. Turbulence*, vol. 5, p. 18, Jul. 2004.

[75] G. M. Di Cicca, G. Iuso, P. G. Spazzini, and M. Onorato, "Particle image velocimetry investigation of a turbulent boundary layer manipulated by spanwise wall oscillations," *J. Fluid Mech.*, vol. 467, pp. 41–56, Sep. 2002.

[76] L. Agostini, E. Touber, and M. A. Leschziner, "Spanwise oscillatory wall motion in channel flow: Drag-reduction mechanisms inferred from DNS-predicted phase-wise property variations at," *J. Fluid Mech.*, vol. 743, pp. 606–635, Mar. 2014.

[77] H. Zhao, J.-Z. Wu, and J.-S. Luo, "Turbulent drag reduction by traveling wave of flexible wall," *Fluid Dyn. Res.*, vol. 34, no. 3, pp. 175–198, Mar. 2004.

[78] M. Quadrio, P. Ricco, and C. Viotti, "Streamwise-travelling waves of spanwise wall velocity for turbulent drag reduction," *J. Fluid Mech.*, vol. 627, pp. 161–178, May 2009.

[79] M. Quadrio, "The response of wall turbulence to streamwise-traveling waves of spanwise velocity," in *Progress in Turbulence III*. Bertinoro, Italy, 2010.

[80] M. Quadrio and P. Ricco, "The laminar generalized Stokes layer and turbulent drag reduction," *J. Fluid Mech.*, vol. 667, pp. 135–157, Jan. 2011.

[81] F. Auteri, A. Baron, M. Belan, G. Campanardi, and M. Quadrio, "Experimental assessment of drag reduction by traveling waves in a turbulent pipe flow," *Phys. Fluids*, vol. 22, no. 11, Nov. 2010, Art. no. 115103.

[82] M.-X. Zhao, W.-X. Huang, and C.-X. Xu, "Drag reduction in turbulent flows along a cylinder by streamwise-travelling waves of circumferential wall velocity," *J. Fluid Mech.*, vol. 862, pp. 75–98, Mar. 2019.

[83] M. Quadrio, "Drag reduction in turbulent boundary layers by in-plane wall motion," *Philos. Trans. Roy. Soc. London A, Math., Phys. Eng. Sci.*, vol. 369, no. 1940, pp. 1428–1442, Apr. 2011.

[84] T. W. Berger, J. Kim, C. Lee, and J. Lim, "Turbulent boundary layer control utilizing the Lorentz force," *Phys. Fluids*, vol. 12, no. 3, pp. 631–649, Mar. 2000.

[85] J.-H. Lee and H. J. Sung, "Response of a spatially developing turbulent boundary layer to a spanwise oscillating electromagnetic force," *J. Turbulence*, vol. 6, p. N39, Jan. 2005.

[86] K. S. Breuer, J. Park, and C. Henoch, "Actuation and control of a turbulent channel flow using Lorentz forces," *Phys. Fluids*, vol. 16, no. 4, pp. 897–907, Apr. 2004.

[87] J. Pang and K.-S. Choi, "Turbulent drag reduction by Lorentz force oscillation," *Phys. Fluids*, vol. 16, no. 5, pp. L35–L38, May 2004.

[88] K.-S. Choi, T. Jukes, and R. Whalley, "Turbulent boundary-layer control with plasma actuators," *Philos. Trans. Roy. Soc. London A, Math., Phys. Eng. Sci.*, vol. 369, no. 1940, pp. 1443–1458, Apr. 2011.

[89] P. Fuaad, M. Baig, and B. Khan, "Turbulent drag reduction using active control of buoyancy forces," *Int. J. Heat Fluid Flow*, vol. 61, pp. 585–598, Oct. 2016.

[90] P. Fuaad, M. Baig, and H. Ahmad, "Drag-reduction in buoyant and neutrally-buoyant turbulent flows over super-hydrophobic surfaces in transverse orientation," *Int. J. Heat Mass Transf.*, vol. 93, pp. 1020–1033, Feb. 2016.

[91] B. A. Khan and M. F. Baig, "Turbulent drag reduction in channel flow using weak-pressure forcing," in *Advances in Computation, Modeling and Control of Transitional and Turbulent Flows*. Singapore: World Scientific, 2016, pp. 195–203.

[92] Y. Du, V. Symeonidis, and G. E. Karniadakis, "Drag reduction in wall-bounded turbulence via a transverse travelling wave," *J. Fluid Mech.*, vol. 457, pp. 1–34, Apr. 2002.

[93] G. E. Karniadakis and K. S. Choi, "Mechanisms on transverse motions in turbulent wall flows," *Annu. Rev. Fluid Mech.*, vol. 35, pp. 45–62, Jan. 2003.

[94] W. Schoppa and F. Hussain, "Genesis of longitudinal vortices in near-wall turbulence," *Meccanica*, vol. 33, pp. 489–501, Oct. 1998.

[95] Y. Hong, W. Wu, and B. Fan, "Reynolds stress in the turbulent channel flow controlled by spanwise travelling wave Lorentz force," *J. Harbin Inst. Technol.*, vol. 47, pp. 88–93, Oct. 2015.

[96] L. P. Huang, "Mechanisms for drag reduction in turbulent wall flows utilizing spanwise motions," Ph.D. dissertation, Nanjing Univ. Sci. Technol., Nanjing, China, 2012.

[97] L. P. Huang and B. C. Fan, "Effect of wave number of spanwise travelling wave-like lorentz force on wall turbulent control," *J. Astronaut.*, vol. 33, pp. 305–310, Mar. 2012.

[98] L. P. Huang, K. S. Choi, and B. C. Fan, "Formation of low-speed ribbons in turbulent channel flow subject to a spanwise travelling wave," *J. Phys., Conf. Ser.*, vol. 318, no. 2, Dec. 2011, Art. no. 022027.

[99] P. Xu and K. S. Choi, "Boundary layer control for drag reduction by Lorentz forcing," in *Proc. IUTAM Symp. Flow Control MEMS*, vol. 7, 2008, pp. 259–265.
[100] R. D. Whalley and K. S. Choi, "Turbulent boundary-layer control with plasma spanwise travelling waves," *Exp. Fluids*, vol. 55, p. 16, Aug. 2014.
[101] Q. Tong, G. Peng, L. Nan-Sheng, and L. Xi-Yun, "Turbulent boundary layer control via a streamwise travelling wave induced by an external force," *Chin. Phys. Lett.*, vol. 25, no. 10, pp. 3700–3703, Oct. 2008.
[102] L. Huang, B. Fan, and G. Dong, "Turbulent drag reduction via a transverse wave traveling along streamwise direction induced by Lorentz force," *Phys. Fluids*, vol. 22, no. 1, Jan. 2010, Art. no. 015103.
[103] S. Kang and H. Choi, "Active wall motions for skin-friction drag reduction," *Phys. Fluids*, vol. 12, no. 12, pp. 3301–3304, Dec. 2000.
[104] M. Itoh, S. Tamano, K. Yokota, and S. Taniguchi, "Drag reduction in a turbulent boundary layer on a flexible sheet undergoing a spanwise traveling wave motion," *J. Turbulence*, vol. 7, p. N27, Jan. 2006.
[105] S. Tamano and M. Itoh, "Drag reduction in turbulent boundary layers by spanwise traveling waves with wall deformation," *J. Turbulence*, vol. 13, p. N9, Jan. 2012.
[106] N. Tomiyama and K. Fukagata, "Direct numerical simulation of drag reduction in a turbulent channel flow using spanwise traveling wave-like wall deformation," *Phys. Fluids*, vol. 25, no. 10, Oct. 2013, Art. no. 105115.
[107] S. Klumpp, M. Meinke, and W. Schröder, "Drag reduction by spanwise transversal surface waves," *J. Turbulence*, vol. 11, p. N22, Jan. 2010.
[108] S. Klumpp, M. Meinke, and W. Schröder, "Friction drag variation via spanwise transversal surface waves," *Flow Turbulence Combust*, vol. 87, no. 1, pp. 33–53, Jul. 2011.
[109] S. R. Koh, P. Meysonnat, M. Meinke, and W. Schröder, "Drag reduction via spanwise transversal surface waves at high Reynolds numbers," *Flow Turbulence Combust*, vol. 95, no. 1, pp. 169–190, Jul. 2015.
[110] S. Koh, P. Meysonnat, V. Statnikov, M. Meinke, and W. Schröder, "Dependence of turbulent wall-shear stress on the amplitude of spanwise transversal surface waves," *Comput. Fluids*, vol. 119, pp. 261–275, Sep. 2015.
[111] P. S. Meysonnat, S. R. Koh, B. Roidl, and W. Schröder, "Impact of transversal traveling surface waves in a non-zero pressure gradient turbulent boundary layer flow," *Appl. Math. Comput.*, vol. 272, pp. 498–507, Jan. 2016.
[112] D. Roggenkamp, W. Jessen, W. Li, M. Klaas, and W. Schröder, "Experimental investigation of turbulent boundary layers over transversal moving surfaces," *CEAS Aeronaut. J.*, vol. 6, no. 3, pp. 471–484, Sep. 2015.
[113] P. S. Meysonnat, D. Roggenkamp, W. Li, B. Roidl, and W. Schröder, "Experimental and numerical investigation of transversal traveling surface waves for drag reduction," *Eur. J. Mech.-B/Fluids*, vol. 55, pp. 313–323, Jan. 2016.
[114] W. F. Li, D. Roggenkamp, T. Hecken, W. Jessen, M. Klaas, and W. Schroder, "Parametric investigation of friction drag reduction in turbulent flow over a flexible wall undergoing spanwise transversal traveling waves," *Exp. Fluids*, vol. 59, p. 18, Jun. 2018.
[115] W. Li, D. Roggenkamp, W. Jessen, M. Klaas, and W. Schröder, "Turbulent drag reduction by spanwise traveling ribbed surface waves," *Eur. J. Mech. B-Fluids*, vol. 53, pp. 101–112, Sep./Oct. 2015.
[116] S. Taneda and Y. Tomonari, "An experiment on the flow around a waving plate," *J. Phys. Soc. Jpn.*, vol. 36, no. 6, pp. 1683–1689, Jun. 1974.
[117] Y. Yao, C.-J. Lu, T. Si, and K. Zhu, "Water tunnel experimental investigation on the drag reduction characteristics of the traveling wavy wall," *J. Hydrodyn.*, vol. 23, no. 1, pp. 65–70, Feb. 2011.
[118] L. Shen, X. Zhang, D. K. P. Yue, and M. S. Triantafyllou, "Turbulent flow over a flexible wall undergoing a streamwise travelling wave motion," *J. Fluid Mech.*, vol. 484, pp. 197–221, Jun. 2003.
[119] R. Nakanishi, H. Mamori, and K. Fukagata, "Relaminarization of turbulent channel flow using traveling wave-like wall deformation," *Int. J. Heat Fluid Flow*, vol. 35, pp. 152–159, Jun. 2012.
[120] H. Ahmad, M. Baig, and P. Fuaad, "Numerical investigation of turbulent-drag reduction induced by active control of streamwise travelling waves of wall-normal velocity," *Eur. J. Mech.-B/Fluids*, vol. 49, pp. 250–263, Jan. 2015.
[121] H. Mamori and K. Fukagata, "Drag reduction by streamwise traveling wave-like Lorenz Force in channel flow," *J. Phys., Conf. Ser.*, vol. 318, no. 2, Dec. 2011, Art. no. 022030.
[122] C.-M. Ho and Y.-C. Tai, "Micro-electro-mechanical-systems (MEMS) and fluid flows," *Annu. Rev. Fluid Mech.*, vol. 30, no. 1, pp. 579–612, Jan. 1998.
[123] A. Huang, J. Lew, Y. Xu, Y.-C. Tai, and C.-M. Ho, "Microsensors and actuators for macrofluidic control," *IEEE Sensors J.*, vol. 4, no. 4, pp. 494–502, Aug. 2004.
[124] J. Kim, "Control of turbulent boundary layers," *Phys. Fluids*, vol. 15, pp. 1093–1105, May 2003.
[125] C.-M. Ho and Y.-C. Tai, "REVIEW: MEMS and its applications for flow control," *J. Fluids Eng.*, vol. 118, no. 3, pp. 437–447, Sep. 1996.
[126] H. Suzuki, N. Kasagi, and Y. Suzuki, "Active control of an axisymmetric jet with distributed electromagnetic flap actuators," *Exp. Fluids*, vol. 36, no. 3, pp. 498–509, Mar. 2004.
[127] A. Pimpin, Y. Suzuki, and N. Kasagi, "Microelectrostrictive actuator with large out-of-plane deformation for flow–control application," *J. Microelectromech. Syst.*, vol. 16, no. 3, pp. 753–764, Jun. 2007.
[128] L. N. Cattafesta and M. Sheplak, "Actuators for active flow control," *Annu. Rev. Fluid Mech.*, vol. 43, pp. 247–272, Jan. 2011.
[129] T. Yeom, T. W. Simon, M. Zhang, M. T. North, and T. Cui, "High frequency, large displacement, and low power consumption piezoelectric translational actuator based on an oval loop shell," *Sens. Actuators A, Phys.*, vol. 176, pp. 99–109, Apr. 2012.
[130] L. Lampani, R. Grillo, and P. Gaudenzi, "Finite element models of piezoelectric actuation for active flow control," *Acta Astronaut.*, vol. 71, pp. 129–138, Feb. 2012.
[131] R. Mani, D. C. Lagoudas, and O. K. Rediniotis, "Active skin for turbulent drag reduction," *Smart Mater. Struct.*, vol. 17, no. 3, Jun. 2008, Art. no. 035004.
[132] A. Phoenix, V. V. N. Malladi, and P. A. Tarazaga, "Traveling wave phenomenon through piezoelectric actuation of a free-free cylindrical tube," in *Proc. ASME Conf. Smart Mater., Adapt. Struct. Intell. Syst.*, New York, NY, USA, 2016.
[133] K. Li, J. Liu, R. Yang, W. Chen, L. Zhang, and Y. Liu, "A trace redundant lubrication piezoelectric microjet for bearing system," *IEEE/ASME Trans. Mechatronics*, vol. 23, no. 5, pp. 2263–2272, Oct. 2018.
[134] O. H. Wehrmann, "Reduction of velocity fluctuations in a Kármán vortex street by a vibrating cylinder," *Phys. Fluids*, vol. 8, no. 4, pp. 760–761, 1965.
[135] J. M. Wiltse and A. Glezer, "Manipulation of free shear flows using piezoelectric actuators," *J. Fluid Mech.*, vol. 249, pp. 261–285, Apr. 1993.
[136] E. F. Crawley and J. De Luis, "Use of piezoelectric actuators as elements of intelligent structures," *AIAA J.*, vol. 25, no. 10, pp. 1373–1385, Oct. 1987.
[137] D. J. Bell, T. J. Lu, N. A. Fleck, and S. M. Spearing, "MEMS actuators and sensors: Observations on their performance and selection for purpose," *J. Micromech. Microeng.*, vol. 15, no. 7, pp. S153–S164, Jul. 2005.
[138] L. N. Cattafesta, III, S. Garg, and D. Shukla, "Development of piezoelectric actuators for active flow control," *AIAA J.*, vol. 39, pp. 1562–1568, Jan. 2001.
[139] D. Haller, A. Paetzold, N. Losse, S. Neiss, I. Peltzer, W. Nitsche, R. King, and P. Woias, "Piezo-polymer-composite unimorph actuators for active cancellation of flow instabilities across airfoils," *J. Intell. Mater. Syst. Struct.*, vol. 22, no. 5, pp. 461–474, Mar. 2011.
[140] J. Mathew, Q. Song, B. V. Sankar, M. Sheplak, and L. N. Cattafesta, "Optimized design of piezoelectric flap actuators for active flow control," *AIAA J.*, vol. 44, no. 12, pp. 2919–2928, Dec. 2006.
[141] S. A. Jacobson and W. C. Reynolds, "Active control of streamwise vortices and streaks in boundary layers," *J. Fluid Mech.*, vol. 360, pp. 179–211, Apr. 1998.
[142] S. Kumar, W. Reynolds, and T. Kenny, "MEMS based transducers for boundary layer control," in *IEEE Int. MEMS Conf. 12th IEEE Int. Conf. Micro Electro Mech. Syst. Tech. Dig.*, Jan. 1999, pp. 135–140.
[143] A. Seifert, S. Eliahu, D. Greenblatt, and I. Wygnanski, "Use of piezoelectric actuators for airfoil separation control," *AIAA J.*, vol. 36, pp. 1535–1537, Jan. 1998.
[144] R. F. Blackwelder, D. Liu, and W. Jeon, "Velocity perturbations produced by oscillating delta wing actuators in the wall region," *Exp. Therm. Fluid Sci.*, vol. 16, nos. 1–2, pp. 32–40, Jan. 1998.
[145] W. . .-P. Jeon and R. F. Blackwelder, "Perturbations in the wall region using flush mounted piezoceramic actuators," *Exp. Fluids*, vol. 28, no. 6, pp. 485–496, Jun. 2000.
[146] X.-B. Zheng, N. Jiang, and H. Zhang, "Predetermined control of turbulent boundary layer with a piezoelectric oscillator," *Chin. Phys. B*, vol. 25, no. 1, Jan. 2016, Art. no. 014703.

[147] J.-X. Bai, N. Jiang, X.-B. Zheng, Z.-Q. Tang, K.-J. Wang, and X.-T. Cui, "Active control of wall-bounded turbulence for drag reduction with piezoelectric oscillators," *Chin. Phys. B*, vol. 27, no. 7, Jul. 2018, Art. no. 074701.

[148] H. Bai, Y. Zhou, W. Zhang, S. Xu, Y. Wang, and R. Antonia, "Active control of a turbulent boundary layer based on local surface perturbation," *J. Fluid Mech.*, vol. 750, pp. 316–354, Jul. 2014.

[149] H. L. Bai, Y. Zhou, W. G. Zhang, and R. A. Antonia, "Streamwise vortices and velocity streaks in a locally drag–reduced turbulent boundary layer," *Flow Turbulence Combust*, vol. 100, no. 2, pp. 391–416, Mar. 2018.

[150] M. B. Mansoor, N. Reuther, S. Köble, M. Gérard, H. Steger, P. Woias, and F. Goldschmidtböing, "Parametric modeling and experimental characterization of a nonlinear resonant piezoelectric actuator designed for turbulence manipulation," *Sens. Actuators A, Phys.*, vol. 258, pp. 14–21, May 2017.

[151] M. Bin Mansoor, S. Koeble, P. Woias, and F. Goldschmidtboeing, "Design and optimization of nonlinear oscillators for drag reduction on airfoils," in *Proc. IEEE 29th Int. Conf. Micro Electro Mech. Syst. (MEMS)*, Jan. 2016.

[152] M. Mansoor, S. Köble, T. Wong, P. Woias, and F. Goldschmidtböing, "Design, characterization and sensitivity analysis of a piezoelectric ceramic/metal composite transducer," *Micromachines*, vol. 8, no. 9, p. 271, Sep. 2017.

[153] P. F. Musgrave, V. V. N. S. Malladi, and P. A. Tarazaga, "Generation of traveling waves in a 2D plate for future drag reduction manipulation," in *Proc. 34th IMAC Conf. Expo. Struct. Dyn.*, Orlando, FL, USA, 2016.

[154] V. V. S. Malladi, M. Albakri, and P. A. Tarazaga, "An experimental and theoretical study of two-dimensional traveling waves in plates," *J. Intell. Mater. Syst. Struct.*, vol. 28, no. 13, pp. 1803–1815, Aug. 2017.

[155] L. Zhang, X. Shan, X. Zhang, and T. Xie, "A method for reducing the drag of the ship shaped wall by using piezoelectric ceramic vibrators," *IEEE Access*, vol. 7, pp. 13295–13303, 2019.

[156] M. Papila, M. Sheplak, and L. N. Cattafesta, "Optimization of clamped circular piezoelectric composite actuators," *Sens. Actuators A, Phys.*, vol. 147, no. 1, pp. 310–323, Sep. 2008.

[157] D. Haller, A. Paetzold, N. Goldin, S. Neiss, F. Goldschmidtboeing, W. Nitsche, R. King, and P. Woias, "Cymbal type piezo-polymer-composite actuators for active cancellation of flow instabilities on airfoils," in *Proc. 16th Int. Solid-State Sens., Actuators Microsyst. Conf.*, Jun. 2011.

[158] T. Segawa, Y. Kawaguchi, Y. Kikushima, and H. Yoshida, "Active control of streak structures in wall turbulence using an actuator array producing inclined wavy disturbances," *J. Turbulence*, vol. 3, p. N15, Jan. 2002.

[159] Y. Li and M. Gaster, "Active control of boundary-layer instabilities," *J. Fluid Mech.*, vol. 550, pp. 185–205, Feb. 2006.

[160] H. Rebbeck and K.-S. Choi, "A wind-tunnel experiment on real-time opposition control of turbulence," *Phys. Fluids*, vol. 18, no. 3, Mar. 2006, Art. no. 035103.

[161] L. V. Lorang, B. Podvin, and P. Le Quere, "Application of compact neural network for drag reduction in a turbulent channel flow at low Reynolds numbers," *Phys. Fluids*, vol. 20, no. 4, Apr. 2008, Art. no. 045104.

[162] C. Lee, J. Kim, and H. Choi, "Suboptimal control of turbulent channel flow for drag reduction," *J. Fluid Mech.*, vol. 358, pp. 245–258, Mar. 1998.

[163] M. M. Zhang, L. Cheng, and Y. Zhou, "Closed-loop controlled vortex-airfoil interactions," *Phys. Fluids*, vol. 18, no. 4, Apr. 2006, Art. no. 046102.

[164] J. Kim and T. R. Bewley, "A linear systems approach to flow control," *Annu. Rev. Fluid Mech.*, vol. 39, pp. 383–417, Jan. 2007.

[165] T. R. Bewley, P. Moin, and R. Temam, "DNS-based predictive control of turbulence: An optimal benchmark for feedback algorithms," *J. Fluid Mech.*, vol. 447, pp. 179–225, Nov. 2001.

[166] C. Lee, J. Kim, D. Babcock, and R. Goodman, "Application of neural networks to turbulence control for drag reduction," *Phys. Fluids*, vol. 9, no. 6, pp. 1740–1747, Jun. 1997.

[167] N. Kasagi, Y. Suzuki, and K. Fukagata, "Microelectromechanical systems–based feedback control of turbulence for skin friction reduction," *Annu. Rev. Fluid Mech.*, vol. 41, no. 1, pp. 231–251, Jan. 2009.

[168] Y. Zhou and H. Bai, "Recent advances in active control of turbulent boundary layers," *Sci. China Phys. Mech. Astron.*, vol. 54, no. 7, pp. 1289–1295, Jul. 2011.

[169] S. L. Brunton and B. R. Noack, "Closed-loop turbulence control: Progress and challenges," *Appl. Mech. Rev.*, vol. 67, Sep. 2015, Art. no. 050801.

[170] Y. Zhou, Z. X. Qiao, and Z. Wu, "Active skin friction drag reduction using different schemes," in *Proc. 3rd Symp. FSSIC*, Perth, WA, Australia, 2016.

[171] Z. X. Qiao, Y. Zhou, and Z. Wu, "Turbulent boundary layer under the control of different schemes," *Philos. Trans. Roy. Soc. London A, Math., Phys. Eng. Sci.*, vol. 473, no. 2202, Jun. 2017, Art. no. 20170038.

LU ZHANG was born in Shandong, China, in 1988. She received the B.E. degree from the School of Mechanical Engineering, Shandong University of Technology, in 2012, and M.E. degrees from the School of Mechatronics Engineering, Harbin Institute of Technology, China, in 2015. She is currently the Ph.D. degree with the Harbin Institute of Technology, China. Her research interests include turbulent drag reduction and ultrasonic vibration.

XIAOBIAO SHAN was born in Fuzhou, Jianxi, China, in 1977. He received the B.E. degree from the School of Automotive Engineering, Harbin Institute of Technology, in 2001, and the M.E. and Ph.D. degrees from the School of Mechatronics Engineering, Harbin Institute of Technology, in 2004 and 2008, respectively. He is currently an Associate Professor with the School of Mechatronics Engineering, Harbin Institute of Technology. His research interests include energy harvesting, ultrasonic-assisted wire drawing, nanogenerator, and ultrasonic vibration.

TAO XIE was born in 1965. He received the B.E. degree from the Department of Precision Instrumentation Harbin Institute of Technology, in 1987, the M.E. degree from the School of Astronautics, Harbin Institute of Technology, in 1990, and the Ph.D. degree from the School of Mechatronics Engineering, Harbin Institute of Technology, in 2003. Since 2003, he has been a Professor with the School of Mechatronics Engineering, Harbin Institute of Technology. His research interests include ultrasonic-assisted wire drawing, piezoelectric energy harvesting, smart structures, and ultrasonic vibration.